2013

Responses to Low Double-Strand Break Levels in Budding Yeast Meiosis

Scott A. Gaskell
Cleveland State University

RESPONSES TO LOW DOUBLE-STRAND BREAK LEVELS IN BUDDING YEAST

MEIOSIS

SCOTT A. GASKELL

Bachelor of Arts in Biology

Rhode Island College

May, 1998

Submitted in partial fulfillment of requirements for the degree

MASTER OF SCIENCE IN BIOLOGY

at the

CLEVELAND STATE UNIVERSITY

May, 2013

This thesis has been approved for

The Department of Biological, Geological,

And Environmental Sciences and the

College of Graduate Studies by

_____Date:_____

G. Valentin Boerner

Committee Chairperson, Department of BGES

Cleveland State University

_____Date:_____

Crystal M. Weyman

Department of BGES,

Cleveland State University

_____Date:_____

Aaron F. Severson

Department of BGES,

Cleveland State University

ACKNOWLEDGEMENTS

I would like to dedicate this thesis to my father, Richard Gaskell. The example you set shaped my character taught me the joy of intellectual pursuits. Thank you also for the moral support you have provided throughout my graduate school career, without which this thesis might not be possible.

I express special thanks to my brother, Todd Gaskell, who also provided a great deal of moral support throughout my life and especially during graduate school.

Finally, regards to all my friends who supported me as I worked toward the completion of this project.

RESPONSES TO LOW DOUBLE-STRAND BREAK LEVELS IN BUDDING YEAST MEIOSIS

SCOTT A. GASKELL

ABSTRACT

During meiosis, one round of DNA replication is followed by two rounds of chromosome segregation, producing four haploid gametes from each diploid precursor cell. Self-inflicted DNA double-strand breaks (DSBs) occur in prophase of meiosis I. A subset of DSBs are repaired using the homologous chromosome as template for homologous recombination, generating crossovers/chiasmata. When processing of DSBs is defective, the recombination checkpoint delays onset of the first meiotic cell division. Here, I have investigated mechanisms by which the budding yeast *S. cerevisiae* responds to low levels of initiating DSBs. A novel checkpoint is identified that is specifically triggered by low DSB levels, but not a lack thereof. This checkpoint is mediated by widely-conserved meiotic checkpoint ATPase Pch2. I propose that during normal meiosis, this low DSB checkpoint delays progress through meiosis until threshold levels of DSBs have been reached. Using genetic approaches, I have also identified three pathways by which the viability of gametes formed during low-DSB meiosis can be improved. Accordingly, (i) higher temperatures, (ii) abrogation of DSB-dependent histone H2A phosphorylation and (iii) overexpression of chromosome structure protein Hop1 constitute determinants for functional gamete formation at low DSB levels. Together, these findings suggest the existence of several layers that ensure faithful chromosome segregation during meiosis.

TABLE OF CONTENTS

LIST OF FIGURES

LIST OF TABLES

CHAPTER I

INTRODUCTION

1.1 The Meiotic Cell Cycle

Meiosis is a specialized type of cell division in sexually reproducing organisms in which one round of DNA replication is followed by two rounds of chromosome segregation. Meiosis produces four haploid daughter cells from a single diploid parental cell. In metazoans, meiosis generates gametes: sperm in males and ova in females. In the budding yeast *Saccharomyces cerevisiae,* the end product of meiosis is four spores. These four spores are surrounded by a cell wall and are collectively known as a tetrad, or ascus.

The first cell division in meiosis consists of a reductional segregation of homologous chromosomes (homologs). Proper segregation of homologs depends upon the formation of chiasmata. Chiasmata are the physical manifestation of the process of genetic recombination, which generates crossovers. Chiasmata provide physical connections between the homologs, ultimately allowing bipolar chromosome attachment (Fig 1). Without bipolar attachment, chromosomes missegregate, resulting in aneuploid gametes and hence chromosomal abnormalities in offspring upon fertilization. Missegregation is a leading cause of still births and birth defects among humans (Cimini and Degrassi, 2005).

Meiosis I is subdivided into four phases. In prophase I, meiotic recombination occurs
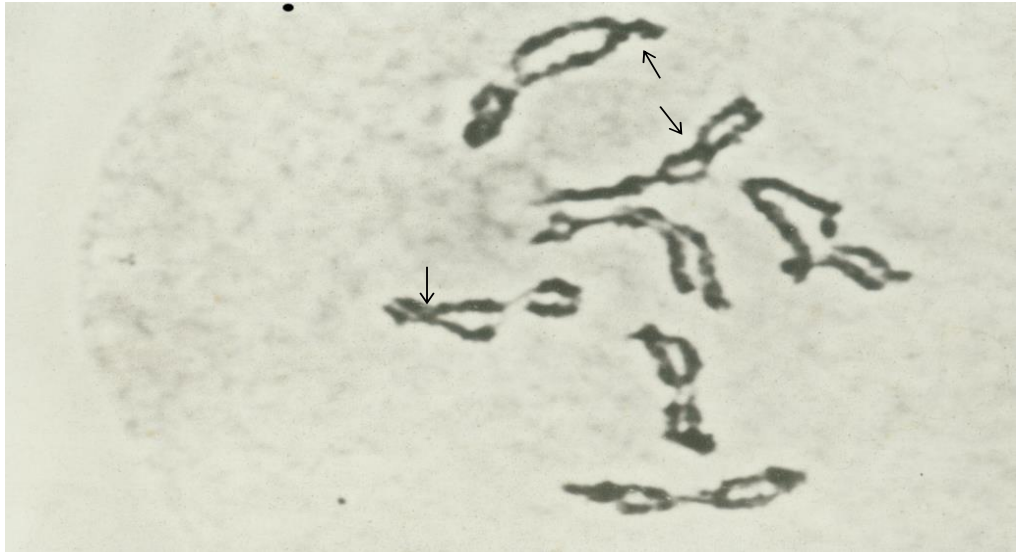
Fig. 1 An electron micrograph of a surface spread of a silver stained diplotene nucleus. Arrows Indicate chiasmata. Image from: http://home.cc.umanitoba.ca/~frist/PLNT3140/l03/l03.3.html

and the chromosomes condense, becoming microscopically visible. During metaphase I, homologs are connected via chiasmata and are aligned at the equator of the cell. Homologs are pulled by spindle fibers toward the opposite poles of the cell in anaphase I. Finally, in telophase I, the chromosomes

begin to decondense. Concomitant with telophase I is cytokinesis, or cell division.

During prophase I, an evolutionarily conserved proteinaceous structure known as the synaptonemal complex (SC) polymerizes between homologs to facilitate recombination, then disassembles to facilitate chromosome segregation. Full formation of the SC results in the close juxtaposition of homologs at a distance of 100 nm, referred to as synapsis. Based on
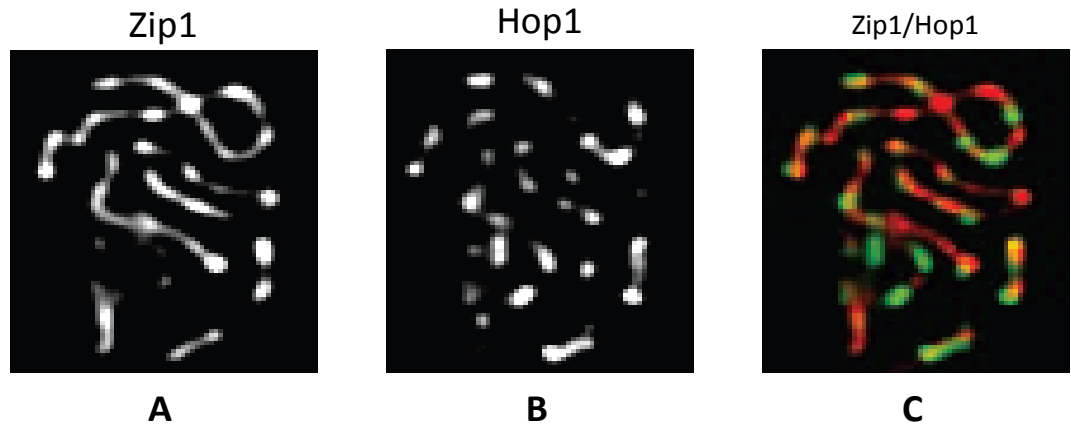
Fig. 2 Immunofluorescence image of a pachytene nuclear spread. A. Immunofluorecence Image stained for SC central element protein Zip1. B. Immunofluorescence image stained For the SC axial element protein Hop1. C. Images A and B merged. Hop1 is green and Zip1 Is red. The two proteins do not colocalize. (Joshi et. Al, 2009)

the status of SC assembly, prophase I is subdivided into five stages. During the leptotene stage, the SC axial elements polymerize as a scaffold along the length of the conjoined sister chromatids. In yeast, axial elements are comprised of the proteins Red1 and Hop1. During the zygotene phase, the central element of the SC, of which the coiled-coil yeast protein Zip1 is a major structural component, begins polymerization from discrete foci. Zip1 spans the 100 nm gap between homologs, forming a ladder-like structure between them (Fig. 2). During the pachytene stage, the SC is fully formed and meiotic recombination is completed. During diplotene, the SC central element depolymerizes and chiasma connections are visible due to physical separation between homologs. Diakinesis follows (reviewed in Hunter, 2006).

1.2 Meiotic recombination:

In parallel with SC formation, meiotic recombination is initiated and completed (Padmore and Kleckner, 1991). Meiotic CO recombination entails creating self-induced double strand breaks (DSBs) followed by the DSB repair events that result in crossovers. DSBs can be repaired through the process of homologous recombination either with the sister chromatid or the homolog. In meiosis, repair occurs preferentially with the homolog. A side effect of crossing over is the exchange of regions of genetic material between homologs, generating new allele combinations along a given chromosome and thus genetic diversity in offspring.

DSB formation is catalyzed by the meiosis-specific type II topoisomerase Spo11 (Keeney et. al, 1997). Spo11's catalytic center performs a nucleophilic attack on the phosphodiester backbone of DNA and becomes covalently attached to the 5' end of the DSB as an integral part of the process of DSB formation (Diaz et. al, 2002). Spo11 acts as a dimer in a complex that consists of at least 11 proteins (reviewed in Hunter, 2006). Among the proteins required for DSB formation is the MRX complex. The MRX complex consists of three proteins (Mre11, Rad50, and Xrs2) and is required for DSB repair via homologous recombination (reviewed in Krogh and Symington, 2004). Though they are not a part of the Spo11 complex, the SC axis proteins Red1 and Hop1 are also required for wild type levels of DSBs. The covalently bound Spo11 is removed from the DSB with a short oligonucleotide via an endonucleolytic cleavage by the Mre11 subunit of the MRX complex. In a process called resection, an exonuclease removes bases from the 5' end of the DSB, producing a 3' single stranded tail (reviewed in Krogh and Symington, 2004).

Following resection, the eukaryotic RecA homologues Dmc1 and Rad51 associate with the 3' end of the resected DSB, displacing the single strand binding protein RPA (Haruta et al., 2006). The resected 3' single stranded overhang invades an intact homologous DNA

template at the allelic position, usually the sister chromatid in mitosis and the homolog in meiosis (Schwacha and Kleckner, 1997; Bzymek and Hunter, 2010). Once a homologous sequence is identified, a DNA polymerase is thought to initiate extension of the invading strand. This strand invasion intermediate may mature into a double Holliday junction
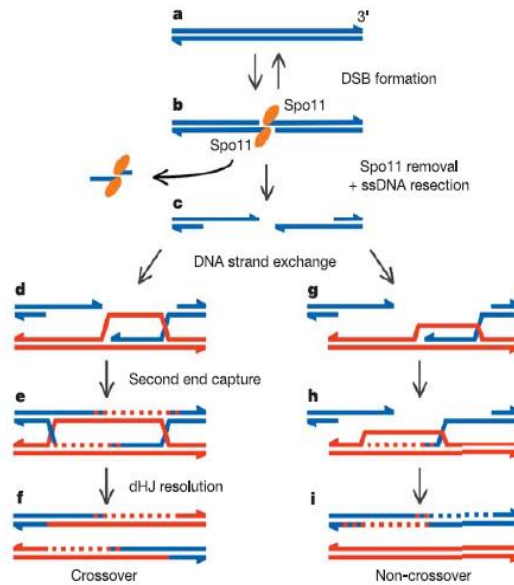
Fig. 3 Events in Meiotic recombination: a-c) The Spo11 complex binds to DNA and catalyzes a DSB. Spo11 is removed with an oligonuclotide and the 5' ends are degraded. Rad51 and Dmc1 bind the resulting 3' single stranded tails. d-f) The single stranded tail invades the homolog and scans for homology. DNA synthesis occurs and the second end is captured; The ends are ligated to form a dHJ. The dHJ is resolved by a resolvase , resulting in a CO. g-i) A NCO is formed through aSynthesis-dependent strand annealing pathway. (Neale and Keeney, 2006)

via annealing of the second end with the same homolog and ligation of both ends (Fig. 3). Double Holliday junctions (DHJ) are resolved by DHJ resolvases resulting in the exchange extensive regions of DNA between homologs (Tay and Wu, 2010).

Alternatively to being processed into a CO with the homolog or sister chromatid, a DSB can also be processed into non-crossover. Non-crossover products involve smaller scale local genetic exchange, without the exchange of flanking chromosome arms. Non-crossovers are likely produced via a synthesis dependent single strand annealing mechanism (McMahill et. al, 2007). The consequence may be gene conversion, which results from the

5

exchange of a chromosomal stretch. These are detected as aberrant non-Mendelian 3:1 segregation of markers instead of the expected 2:2 pattern.

1.3 Establishment of the interhomolog bias

Repair of self-induced DSBs during meiosis is directed toward the homolog. In addition to its role in DSB formation, the SC lateral element protein Hop1 is intimately involved in repair partner choice in meiosis. Hop1 is phosphorylated by the yeast homologues of the mammalian phosphatidylinositol-3-OH kinase related kinases ATM and ATR, Mec1 and Tel1 (Carballo et al.,2008). In a mechanism that is poorly understood, Hop1 also promotes normal levels of DSBs; in a *hop1* deletion strain, DSBs are reduced to 4% of WT levels (Niu et.al., 2005).

Hop1 phosphorylation promotes the recruitment, dimerization, and self-phosphorylation of Mek1, a protein kinase (Niu et. al, 2005). One of the targets of activated Mek1 is Rad54, a binding partner of the mitotic strand invasion protein Rad51. In mitosis, Rad 51 and 54 together promote homologous recombination with the sister chromatid (Sugawara et al., 2003). In meiosis, phosphorylation of Rad 54 prevents it from associating with Rad51, hence preventing strand invasion with the sister chromatid. Phosphorylation of Rad54 by Mek1, in addition to phosporylation of other possible targets, produces a barrier to intersister repair, creating a strong bias toward DSB repair with the homolog (Niu et al., 2009). By ensuring interhomolog repair, this assures crossover formation and thus promotes proper chromosome segregation in meiosis I.

Hop1 function in interhomolog repair can be separated from its role in DSB formation. Accordingly, in the absence of Hop1, DSBs are reduced and the remaining DSBs are rapidly repaired with the sister chromatid (Woltering et al., 2000; Niu et. al, 2005). When

Tel1/Mec1 phosphorylation sites in Hop1 are eliminated, by contrast, DSBs form at normal

levels and progress to sister repair (Carballo et. al, 2008).

1.4 Histone H2A and its role in meiotic recombination

Meiosis-specific structural proteins such as Hop1, as well as ubiquitous chromosomal

proteins, play a role in chromosome function during meiosis. Histones are proteins around
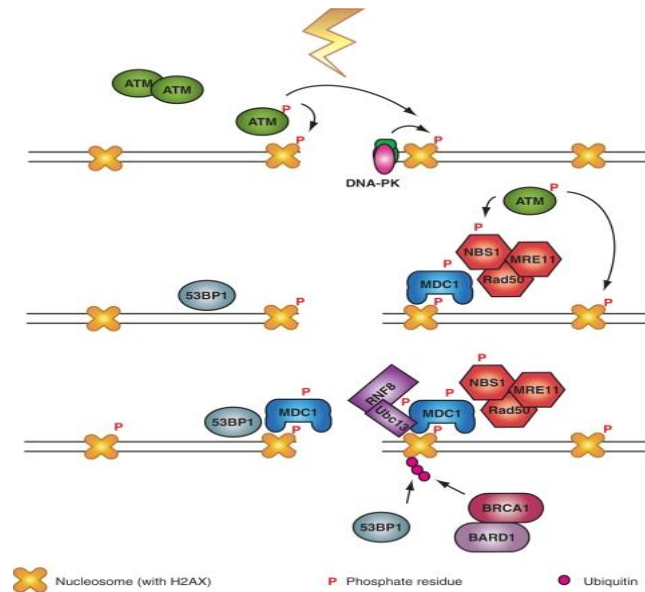
Fig. 4 γ-H2AX coordinates DDR signaling. H2AX is phosphorylated byATM or DNA-PK and subsequently MDC1 is recruited. The MRN binds and further activates ATM. This generates a positive feedback loop in which ATM further phosphorylates H2AX and the chromatin modifications required for the recruitment of 53BP1 occur. The signal cascade results in recruitment of RNF8 to phosphorylated MDC1 and the polyubiquitinylation of H2AX to recruit BRCA1/BARD1 (Kinner et. al., 2008)

which DNA is wound, condensing the genome to chromatin. The basic unit of chromatin is

the nucleosome, which is composed of an octamer of histones; a pair of dimers of H2A and

H2B and a heterotetramer of H3 and H4 proteins. Approximately 146 base pairs of DNA is

wrapped around the core nucleosome with a stretch of DNA between core particles.

(Richmond et al, 1984)

In mammals, a variant of histone H2A, H2AX, is important in the cellular response to

7

DNA damage. In the presence of DNA double strand breaks damage, one of the first responses is the addition of a phosphate group to serine 139 in the carboxy-terminal tail of H2AX (Rogakou et al., 1998). In mammals, the domains of H2AX phosphorylation stretch for several megabases surrounding the DSB site (~50kb in yeast). Phosphorylation of H2AX is performed by the ATM and ATR in mammals (Mec1 and Tel1 in *S. cerevisiae*) (Burma et. al, 2001). H2AX phosphorylation attracts foci of DNA damage repair factors such as Rad50, a member of the DSB processing MRN complex (MRX in *S. cerevisiae*, see above), Rad51, BRCA1, and MDC1 to the DSB site (Paull et al., 2000; Stucki et al., 2005). Nbs1, another member of the MRN complex, directly associates with phosphorylated H2AX via a BRCT repeat domain (Kobayashi et. al, 2002). The MRN complex recruits ATM, which in turn phosphorylates and activates checkpoint factors such as Chk2 (Fig. 4) (Matsuoka et al., 2000).

In male mouse meiosis, H2AX is rapidly phosphorylated in response to the Spo11 catalyzed, self-inflicted DSBs that initiate meiotic recombination (Mahadevaiah et al., 2001). Over time, gamma H2AX disappears, presumably as DNA damage is repaired and a second round of H2AX phosphorylation occurs in the unsynapsed regions of the sex chromosomes. This second, ATM-dependent round of H2AX phosphorylation remodels chromatin and silences transcription in the sex chromosomes (Mahadevaiah et al., 2001; Fernandez-Capitello, 2003).

In mammals, there are multiple H2A variants of which H2AX is one. In budding yeast, however, there are two identical loci that encode histone H2A known as *HTA1* and *HTA2* (Choe et. al, 1982). Both loci encode identical H2A which contains a consensus site on the C-terminal tail, Serine 129, which matches the function of the vertebrate phosphoinositol-3-kinase kinase (PIKK) site. S129 is phosphorylated in response to DSBs

8

(Downs et. al, 2000). When S129 at both H2A loci is mutated, yeast cells become hypersensitive to DSB inducing agents such as methyl methane-sulfonate (MMS), highlighting its importance in the DNA damage response (Tsukuda et al., 2005).

In *S. cerevisiae* mitosis, H2A phosphorylation is required for full recruitment of the adaptor protein Rad9, a 53BP1 ortholog (Jahaveri et al., 2006). In the absence of H2A, phosphorylation activation of the checkpoint kinase Rad53 is deficient. There is a marked delay in G1 in response to DNA damage, and cells with non-phosphorylatable H2A are defective in the DNA damage checkpoint (Jahaveri et al., 2006).

During mitotic growth in yeast, DSB repair requires both the MRX complex (see above) and the chromatin remodeling complex INO80. The INO80 complex is recruited to sites of DNA damage by phosphorylated H2A, where it is required for damage-induced sister chromatid recombination (Kawashima et. al, 2007). INO80 fails to localize to DNA damage sites in mutants which carry non-phosphorylatable alleles of H2A (Van Atticum et al. 2004).

While H2A's role in DSB repair and checkpoint function has been studied in yeast mitosis and H2AX phosphorylation has been observed in mammalian meiosis, its role in yeast meiosis remains unclear.

1.5 Meiotic checkpoints: the role of Pch2 in monitoring processes that govern crossover formation

Checkpoints halt cell cycle progress unless certain conditions are met to ensure proper cell maturation and division. When a checkpoint is triggered, if the stimulus is transient, it is observed as a delay. If the stimulus remains for extended periods of time, however, the checkpoint is manifests as a more extended arrest. The mitotic DNA damage checkpoint, for example, prevents the cell from progressing from G2 to M phase in the presence of DNA

damage (reviewed in Cuddihy and O'Connell, 2003). This allows appropriate time for all DNA lesions to be repaired before the onset of chromosome condensation and separation in prophase and anaphase, respectively. The DNA damage checkpoint thus prevents possible aberrations during chromosome segregation.

When proteins that mediate checkpoints are mutated, cells pass to the subsequent phase of the cell cycle without meeting checkpoint conditions. Pch2, or pachytene checkpoint 2 protein, is a meiosis specific protein that is thought to monitor the proper formation of the SC/chromosome synapsis, and/or the presence of unrepaired recombination intermediates (San-Segundo and Roeder, 1999; Ho and Burgess, 2011). While Pch2 is meiosis specific, Rad17, Rad24, Mec1, and Tel1 are DNA damage checkpoint proteins that are shared among mitosis and meiosis and collaborate with Pch2 (Ho and Burgess, 2011).

Pch2 is a member of the AAA+ ATPase family of proteins. Pch2 is evolutionarily conserved and plays a role in monitoring synapsis in several organisms. In *D. melanogaster*, Pch2 mediates a checkpoint that delays meiotic progression in mutants that display improper SC axis formation (Joyce and McKim, 2010). In *C. elegans*, each chromosome has a region known as a pairing center that promotes homolog synapsis. In females heterozygous for a mutation in the pairing center on the X chromosome, asynapsis of the X chromosome in meiosis I occurs in 60% of meiotic cells. The majority of these meiotic cells, however, are culled from the population though apoptosis; Pch2 is part of the checkpoint that triggers apoptosis in these oocytes and in the absence of Pch2, apoptosis is reduced (Bhalla and Dernburg, 2005).

In *S. cerevisiae*, Pch2 may monitor synapsis and/or DSB repair. In *ZIP1* deletion mutants in which the central element of the SC is absent, cells arrest at the pachytene stage of meiosis. Pch2 is required for this arrest (San-Segundo and Roeder, 1999). Pch2 is also

required for checkpoint function in a sae2 deletion (sae2Δ) background, in which unresected DSBs accumulate. Pch2Δ alleviates the meiotic delay that occurs in a sae2Δ background, suggesting that Pch2 monitors the processing of unresected DSBs. (Wu and Burgess, 2006).

While Pch2 is a meiosis-specific checkpoint component, Rad17 in conjunction with Mec1 monitors DNA damage in both mitosis and meiosis. Rad17 is required for checkpoint function in a *dmc1* mutant background in which resected 3' overhangs accumulate (Ho and Burgess, 2011).

In addition to its checkpoint function, Pch2 mediates crossover placement and SC assembly during WT meiosis; *pch2* deletion at WT DSB levels results in altered Hop1 localization, a lengthening of chromosome axes, and a CO placement that is not interference distributed (Joshi et al. 2009; Zanders and Alani, 2009) i.e. not influenced by the process of CO interference, which ensures that once a CO occurs, a second CO becomes less likely in adjacent regions. If a second crossover between homologous chromosomes occurs, it tends to be maximally spaced. CO interference is mediated by Pch2 in yeast meiosis (Joshi et al. 2009; Zanders and Alani, 2009) At normal DSB levels, Pch2 deletion mutants exhibit altered map distances as measured in centimorgans (percentage of crossovers between loci), showing non-interference distributed CO placement (Zanders and Alani, 2009; S. Gaskell, unpublished data).

It has been proposed that initiation of meiotic recombination triggers a delay in meiotic progression; when recombination initiation-related genes such as *SPO11* and *REC102* are deleted, the onset of the first meiotic division advances (Malone et. al, 2004). . I considered the implications of this observation and wondered whether the delay was mediated by a specific checkpoint. In this work, I employed a budding yeast *spo11* hypomorph strain that produces reduced meiotic DSBs to simulate the conditions of early

meiosis (low DSBs). I determined that a there is a delay in meiotic nuclear divisions relative to high DSB conditions (WT *SPO11*) in the *spo11* hypomorph. I next asked whether a lack of DSBs would trigger an even greater defect and discovered that the delay is activated by low DSBs but not their absence. I examined meiotic progression in a *spo11* hypomorph that was also deficient in the meiosis-specific checkpoint component Pch2 and found that Pch2 mediates the delay I observed at low DSB levels, suggesting that a checkpoint has been activated. Since checkpoints usually function to allow cells time to correct a defect, I investigated whether the delay imparted any growth advantage. At 30ºC, the *spo11* hypomorph exhibited relatively low spore viability. At increased temperature, however, spore viability was markedly increased. I performed a physical analysis of COs at the well-characterized HIS4-LEU2 hotspot under low and high temperature conditions and found that the increase in spore viability was not due to an increase in COs. Since phosphorylated histone H2A is known to function in checkpoint signaling in yeast mitosis and because it is a target of Mec1 and Tel1 (Downs et al., 2000), which also function in the Pch2 pathway (Ho and Burgess, 2011), I next asked whether H2A plays any role in the checkpoint delay I observed. I introduced a mutation that abrogated H2A's phosphorylation site at both H2A loci in a *spo11* hypomorph background. Surprisingly, I found that rather than accelerating meiotic progression as would be expected if a checkpoint component is removed, the *h2a* mutation conferred an additional delay. This delay was reproducible at moderate and high DSB levels. Unexpectedly, I found that the delay conferred by the *h2a* mutation did confer a growth advantage to cells at all DSB levels considered. The overarching theme of this work is the function of checkpoints in wild type meiosis.

CHAPTER II

MATERIALS AND METHODS

2.1 Meiotic time course:

Yeast strains were retrieved from the -80^0C freezer and patched to solid YPG media and incubated at 30ºC for 12 to 16 hours. Strains were streaked for single colonies on YPD media and incubated at 30ºC for 56 hours. Single colonies were inoculated in 4 mL YPD liquid culture and incubated at $30°$C for 26 hours in a roller drum. Cultures were transferred to 150 mL YPA liquid media in a 2L flask and placed in a shaker at $30°$C and 280 rpm for 13 hours. The optical densities (O.D.) of the cultures were measured using spectrophotometer and cultures with an OD value in the range of 1.2 to 1.6 were selected and centrifuged at 4000 rpm for 4 minutes. Cultures were washed in 100 mL liquid sporulation media (SPM) then resuspended in 150 mL SPM liquid media then placed in sterile 2L flasks. Cultures were placed in shaker at 290 rpm and 30ºC for 2 hours. Cultures in were split at 2 hours and half (~70 mL) was replaced in the shaker at 30ºC and half was poured into a second sterile 2L flask and shaken at 280 rpm and higher temperature (33.5ºC or 34.5ºC). Samples were collected at 0, 2, 3, 4, 5, 6, 7, 8, 9, 10, 11, and 24 hour time points and placed in DAPI fix for analysis of nuclear divisions. Separate samples were taken for analysis of spore viability at 24 hours. Fixed samples were observed under a fluorescence microscope at 1000X

13

magnification after staining samples with DAPI and nuclei were observed. Cells were categorized as having 1, 2, and 3 or 4 nuclei. Experiments were performed multiple times due to the inherent variability in nuclear division timing among experiments to verify reproducibility. Results for all individual experiments are listed in the appendicies.

2.2 Tetrad dissection

100 uL of samples taken for spore viability analysis in the meiotic time course protocol were centrifuged and resuspended in zymolyase buffer. Samples were exposed to 5 ul of 20 mg/mL zymolyase enzyme, incubated at 37°C for 30 minutes to digest tetrad cell walls. Tetrads were dissected under a light microscope, four spores were linearly placed on YPD media at regular intervals in a grid pattern. Tetrad dissection plates were incubated at 30ºC for 3 to 4 days, viable spores were counted, and percent viability was calculated.

2.3 Construction of a SPO11 ARS-CEN plasmid

A PCR was performed on VBY 1083 wild-type genomic DNA using SPO11 -390s and +540as primers (below) and Agilent Picomaxx enzyme. The 2.1 kb PCR product was run on a 0.7% agarose gel, excised, and extracted with a Qiagen gel extraction kit. The PCR product was then ligated into the TOPO 2.1 cloning vector. NEB turbo competent bacteria were transformed with the ligation mixture using NEB's 30 second heat shock protocol. The transformation mixture was spread using sterile glass beads on luria broth plates supplemented with 50 ug/mL ampicillin that had been coated with IPTG and XGal. The transformation plates were incubated at 37^{0}C for 16 hours and plasmid extractions were performed on the transformants. The 2.1 kb *SPO11* insert was removed from the TOPO vector with the restriction endonucleases SacI and XhoI. The SacI and XhoI digest was run

on a 0.7% agarose gel and the insert was extracted with a with a Qiagen kit. The Ars Cen plasmid pVBB30 was digested with SacI and XhoI, the digestion mixture was run on a 0.7% gel, and the plasmid backbone was extracted with a Qiagen gel extraction kit. The *SPO11* insert and Ars Cen backbone were ligated together to produce the plasmid S4A with NEB quick ligase.

2.4 Optimization of rich sporulation media

Sporulation of the genetic screen strain SGY 98 was carried out as an initial test on rich sporulation media (Spmr) tris base pH 8.0, Spmr tris pH 7.0, spmr 2% raffinose, spmr supplemented with lysine, and spmr with Poland Springs water, and spmr leu- tris pH 8.0 with Poland springs water. Percentage sporulation was visually estimated under a light microscope. The greatest growth and least sporulation occurred on spmr supplemented with lysine. Lesser growth and greater sporulation occurred on all other plates tested. Visual inspection and examination under UV light, which causes the dityrosine in spore cell walls to fluoresce, indicated that spmr leu- pH 8.0 with Poland Springs water produced the best combination of growth and sporulation. The recipe follows: 0.02% leu- powder; 2% 20g agar; 2% KAcetate; 0.22% east extract; 0.05M tris base pH 8.0; 950 mL Poland Springs H2O

2.5 Competent yeast

Competent yeast cells were prepared according to the Lithium acetate method (Ausubel et al.,2002)

2.6 Yeast transformation

Yeast transformations were performed according the the standardized lithium acetate protocol (Ausubel et al.,2002)

2.7 High efficiency yeast plasmid rescue

Two methods for plasmid extraction from yeast were attempted. Initially, yeast cultures cell walls were disrupted with zymolyase enzyme and the Zymoprep kit protocol was followed. Results were inconsistent so another method was attempted. The protocol outlined below achieved reproducible results and was therefore employed to isolate plasmids from genetic screen candidates. Yeast cultures were grown to saturation overnight at 30ºC overnight in liquid YPD media then centrifuged at 13,200 rpm in 1.5 mL microcentrifuge tubes. The supernatant was decanted. Cells were resuspended in 250 uL of Qiagen buffer P1 with RNAse A was added, and ~250uL of glass beads were added. Samples with glass beads were vortexed on high for 3-5 minutes to disrupt the yeast cell walls. 350uL of Qiagen buffer P2 lysis buffer was added and the samples were inverted several times to mix. The samples were allowed to stand for ~5 minutes. 350 uL of Qiagen buffer N3 was added and gently mixed to precipitate genomic DNA and other cell debris. The samples were centrifuged at 13,200 rpm for 10 minutes to pellet cell debris. The supernatant was applied to Qiagen plasmid prep columns and these were centrifuged for 1 minute at 13,200 rpm. The flow through was discarded. The columns were washed with 750uL of Qiagen buffer PE and centrifuged for 1 minute at 13,200 rpm. The flow through was discarded and the columns were centrifuged for 1 minute at 13,200 rpm to ensure there was no residual buffer PE present. 50uL of Qiagen buffer EB was added directly to the membrane and the columns were placed in clean microcentrifuge tubes. These were allowed to stand for 1 minute. The columns were centrifuged for 1 minute to elute the plasmid DNA. 5 uL of the plasmid

16

preparations produced were used to transform competent DH5α bacteria using the NEB 30 second heat shock protocol.

2.8 *E. coli* transformation

Transformations were performed on NEBα high efficiency competent E. coli according to NEB's 30 second heat shock protocol.

2.9 *E. coli* plasmid DNA extraction

Plasmid extractions were performed according to standardized alkaline protocol (Ausubel et al., 2002)

2.10 Yeast genomic DNA extraction (mitotic)

S. cerevisiae mitotic DNA extractions were performed according to standardized protocol (Ausubel et al., 2002)

2.11 Yeast genomic DNA extraction (meiotic)

S. cerevisiae meiotic DNA extractions were performed according to standardized protocol (Ahuja and Borner, 2011)

2.12 Southern blot

Southern blots were performed using the upward capillary action protocol (Ausubel et al.,2002)

2.13 Genetic Screen for genes that interact with *SPO11* and *PCH2*

Competent yeast were prepared of a *spo11-da pch2Δ* strain (SGY 98) and spo11-da PCH2 strain (SGY 48) according to the lithium acetate method. Separate aliquots of SGY98 were transformed with 5 uL of the Nasmyth library, 1 uL of pVB30, and 5 uL of S4A *SPO11* plasmid. SGY 48 was transformed with 1 uL of pVB30 only. 98 well microtiter dishes of liquid leu- media were inoculated with controls and candidate transformant colonies. Inoculated microtiter dishes were incubated overnight at room temperature on a shaker at 70 rpm. Cells were resuspended with a multipipette and stamped to spmr leu- tris pH 8.0 (hereafter referred to as spmr leu-) and leu- plates with a frogger. The spmr leu- plates were incubated at 30ºC for four days then replica plated to leu- plates supplemented with cycloheximide (leu- cyc plates). Leu- cyc plates were incubated for 24 hours at 30ºC then 24 hours at room temperature on the bench. Growth of any candidates was noted on the leu- cyc plates and the corresponding colony was identified on the leu- backup plate. Candidates were streaked for single colonies on leu- plates and candidates were retested in triplicate following the procedure outlined above.

Glycerol stocks were made of candidates that retested in triplicate and these were accepted as secondary candidates. Samples of secondary candidates were taken from the sporulation plates and were subjected to zymolyase digestion . Tetrads were dissected on solid YPD media and the dissection plates were allowed to incubate at 30ºC for three to four days. Spore viability was calculated and compared to the viability of *spo11-da pch2Δ* strain transformed with S4A, *spo11-da PCH2,* and *spo11-da pch2Δ* controls. Secondary candidates that exhibited rescued spore viability were accepted as final candidates. The Nasmyth plasmids were isolated from yeast with the high efficiency yeast plasmid rescue protocol listed above. Yeast plasmid preparations were used to transform NEB DH5α commercial competent cells to amplify the plasmids and the transformation mix was spread on LB plates

supplemented with 50 ug/mL ampicillin. Single colonies from the bacterial transformation were inoculated into 4 mL 50 ug/mL LB ampicillin liquid and placed in a shaker at 37^0C and 250 rpm for 16 hours. Plasmid DNA extractions were performed and these were sequenced using the Sanger method. Candidate plasmid preparations were used to retransform SGY 98 competent cells. Candidates were retested in triplicate once they had been retransformed into yeast.

2.14 Primers used

Spo11 -390 S
GCAATGGTTAAAGGGTTGCT

Spo11 +540 AS
AGAGGTGCTGATGCTTCGTT

P1
GACATACCAGTCTTCCTCATATGAC

P2
CGACTGCATGATGGTTTTCTTAGG

P10
TTTCTGGTCTTGTTGAACCATCATCTATTTAC

P11
GCATGACATATGTTACCGTTAATTATATACCC

2.15 PCR reaction mixtures (used for all PCRs including Spo11 -390 S and spo11 +540 AS)

Primer 1	3uL
Primer 2	3uL
8mM dNTPs	3uL
10X buffer	3uL
Picomaxx	3uL
Template	1.2uL
NPSF H2O	+16.5 uL
Total	30.0 uL

2.16 PCR Conditions

SPO11 -390 and +540 (*SPO11* plasmid construction)

1. 94°C for 5'
2. 90°C for 40"
3. 60°C for 40"
4. 72°C for 3'
5. 35 cycles
6. 94°C for 40"
7. 60°C for 40"
8. 72°C for 7'
9. 4°C indefinitely

P1 and P2, P10 and P11(*HTA1* and *HTA2* for *h2a* strain construction)

1. 95°C for 2'
2. 95°C for 30"
3. 55°C for 1'
4. 72°C for 2'
5. 35 cycles
6. 72°C for 10'
7. 4°C indefinitely

2.17 Construction of *spo11-da h2a* strains

The α strain VBY 1648 which carried an hta1 and hta2 mutation of Serine 129 to alanine on each allele was mated to the A strain NJY 395 which carried the *spo11-da* mutation marked with the antibiotic G418 (KanMX). The strains were mixed in liquid YPD media, pipetted to YPD solid media, then allowed to mate for 6 hours at 30°C. The mating mix was patched to sporulation media (spm) and incubated at 30°C for five days. The mating mix was suspended in 100uL of zymolyase buffer in a microcentrifuge tube, 10uL of 5mg/mL zymolyase was added, an samples wereincubated 37°C for 30. Tetrads were dissected on solid YPD media incubated for four days at 30°C. The tetrad dissection plates were replica plated to G418, ura-, lys-, leu- and arg- selection media. Since the parental diploid strain was heterozygous for G418 resistance, spores grew in a 2:2 segregation pattern. G418+ colonies

that had properly segregated and had minimal auxotrophies were selected. Yeast genomic DNA extractions were performed on all candidates. PCRs with primer pairs P1 and P2 (*HTA2* locus), P10 and P11(*HTA1* locus) were performed on the genomic DNA preps of the candidates in addition to WT controls. Primer pair P1 and P2 produced a PCR product of 599 bp and P10 and P11 produced a PCR product of 692 bp. The S129A mutation created an Fsp1 site and the PCR products, when digested with Fsp1 produced restriction fragments of 499 bp and 100 bp (P1 and P2) and 527 bp and 165 bp (P10 and P11). The PCR products were digested with Fsp1 and run on a 1.5% agarose gel until sufficiently resolved. Strains that contained both hta1 and hta2 mutations produced the above listed restriction fragments whereas the wild type control remained full length PCR products following Fsp1 digestion. Strains with both *h2a* loci mutations in addition to the *spo11-da* mutation were selected for further use.

CHAPTER III

RESULTS

3.1 <u>Low DSB levels confer a meiotic delay.</u>

While yeast has checkpoints that monitor intermediate defects in DSB processing, no meiotic checkpoint appears to monitor the presence of DSBs. Cells with the catalytically inactive *spo11-Y135F/Y135F* (hereafter *spo11-yf*) mutation progress through meiosis with WT kinetics. I hypothesized that, in wild type meiosis, a checkpoint mediating a transient arrest would be useful to cells following onset of double strand break formation, when cellular DSB levels are low. This checkpoint would allow time for DSBs to accumulate to sufficient levels and/or for recruitment of the DSB repair machinery, ultimately ensuring that each homolog pair receives crossovers as required for proper chromosome segregation in MI. To simulate this early time in meiosis, I chose a spo11 hypomorph mutant in which there is a point mutation of aspartate 290 to alanine and an HA epitope tag (spo11 D290A HA, hereafter referred to as *spo11*-da) that exhibits reduced meiotic DSB activity in vivo of between 4% and 12% wild type levels (Henderson and Keeney, 2004). Using the *spo11*-da strain (SGY 148) and an isogenic wild-type strain (VBY 1083), I monitored nuclear divisions

and hence meiotic progression at appropriate time points after induction of synchronous meiosis (Materials and Methods).

Meiosis is normally monitored at 30ºC. Since some phenotypes are more pronounced at higher or lower temperatures, I performed time courses at a range of temperatures. To ensure that cultures under different conditions are comparable, I began with starter cultures at 30ºC to allow for proper replication then split them, incubating at various temperatures thereafter (in this case at 30ºC, 33.5ºC).

To track nuclear divisions and hence progress in meiosis, cells were stained with DAPI, a DNA specific dye that causes nuclei to fluoresce blue when exposed to UV light. Cells were characterized as having a single nucleus, indicating that the cells were in bona fide prophase I, two nuclei, in which the first nuclear division of meiosis was complete, or four nuclei, in which both the first and second nuclear divisions of meiosis had occurred. Cells with three observable nuclei were considered to have four nuclei, with one nucleus out of focus. Since I was primarily concerned with the efficiency of completion of meiosis I, I cumulatively treated all cells with two, three, and four nuclei as having completed meiosis I. Nuclear divisions were expressed (A) as a percentage of total cells and (B) as a percent of maximum value. Efficiency of nuclear divisions was derived from the maximum percentage of divided nuclei observed at the final time point, while delays in meiotic progression were determined by comparing the time when half of the maximum levels of nuclear divisions had occurred. To determine this, graphs that were normalized for percentage of maximum nuclear divisions were generated and the time at which the curves intersect with the 50% mark was graphically determined. The delay in meiotic progression was calculated by subtracting the 50% entry time for the *spo11-da* culture from that of the wild-type (WT) culture.

23

Cultures were split at the two hour time point to ensure proper progress through S-phase, and thereafter half was incubated at 30ºC and 33.5ºC, respectively. At 30ºC, the *SPO11* wild type (*SPO11*, red) and the *spo11-da* (blue) cultures reached the 50% entry mark at 6.8 hours and 8.6 hours, respectively, indicating a delay in *spo11-da* of ~1.8 hours (Fig 5B). The *SPO11* culture reached peak nuclear divisions of 98.2% and the *spo11-da* culture reached 81% nuclear divisions for efficiency of 83% in the *spoll-da* culture (Fig. 5A)

At 33.5ºC, the *SPO11* (red) and the *spo11*-da (blue) cultures reached the 50% entry mark at 6.8
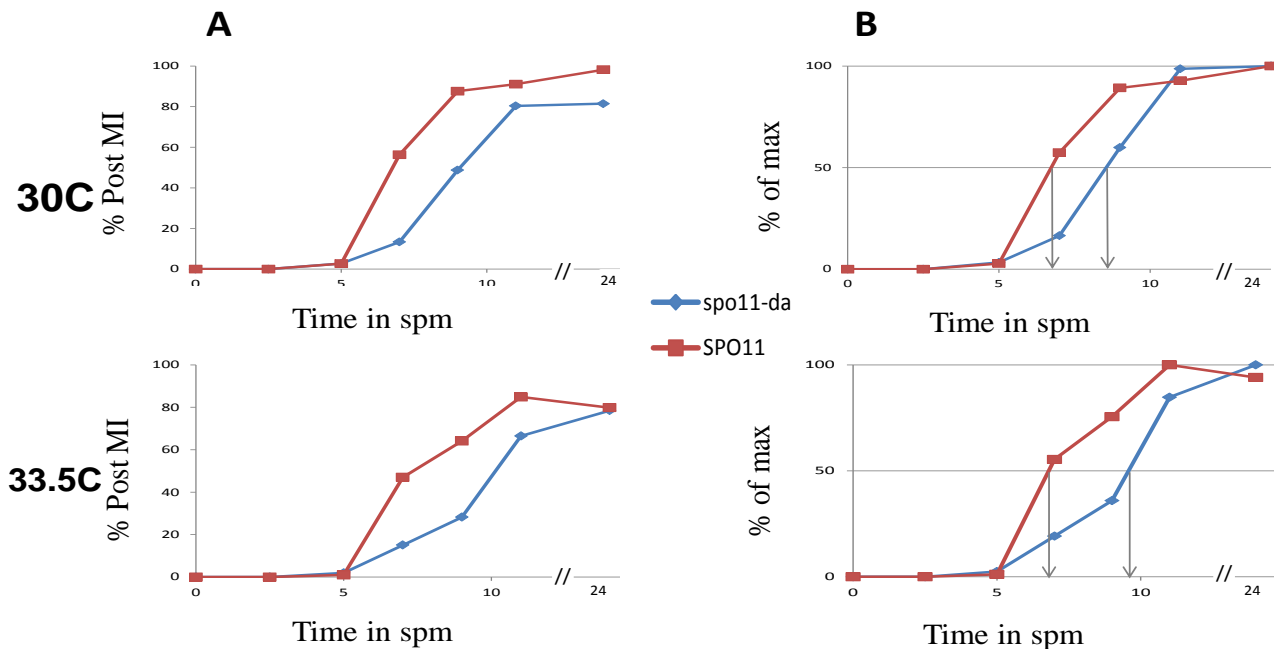
Figure 5. The *spo11-da* mutation confers a delay in meiotic nuclear divisions. Meiotic progression in *SPO11* and *spo11-da* cultures sporulated at both 30C and 33.5C. Meiotic progression was monitored by DAPI staining to determine the number of binucleate (MI) and tetranucleate cells (M2) then graphed as a percentage of total cells. There is a delay in progression of the spo11-da cultures at both temperatures examined. Nuclear divisions were expressed as A. Percent of total cells B. as a percent of maximum. Downward arrows indicate the time at which curves reach the 50% entry mark. Delays were calculated from these 50% entry times.

and 9.6 hours, respectively, indicating a delay of ~2.8 hours in the *spo11*-da (Fig 5B). The *SPO11* culture reached peak nuclear divisions of 80% and the *spo11-da* culture reached 78% nuclear divisions for efficiency of 98% (Fig. 5A)

The delay at 30ºC for three individual experiments was calculated, then the mean was

determined to be 1.9 +/-0.170 hours (mean +/- standard deviation). Only a single experiment

was conducted at 33.5ºC. Further experiments were conducted at 34.5ºC, so no mean could

be calculated at that temperature.

My results demonstrate a marked delay in nuclear divisions in the hypomorphic

spo11-da strain relative to the wild type strain. This suggests the existence of a transient

arrest triggered by low levels of DSBs but not at normal DSB levels.
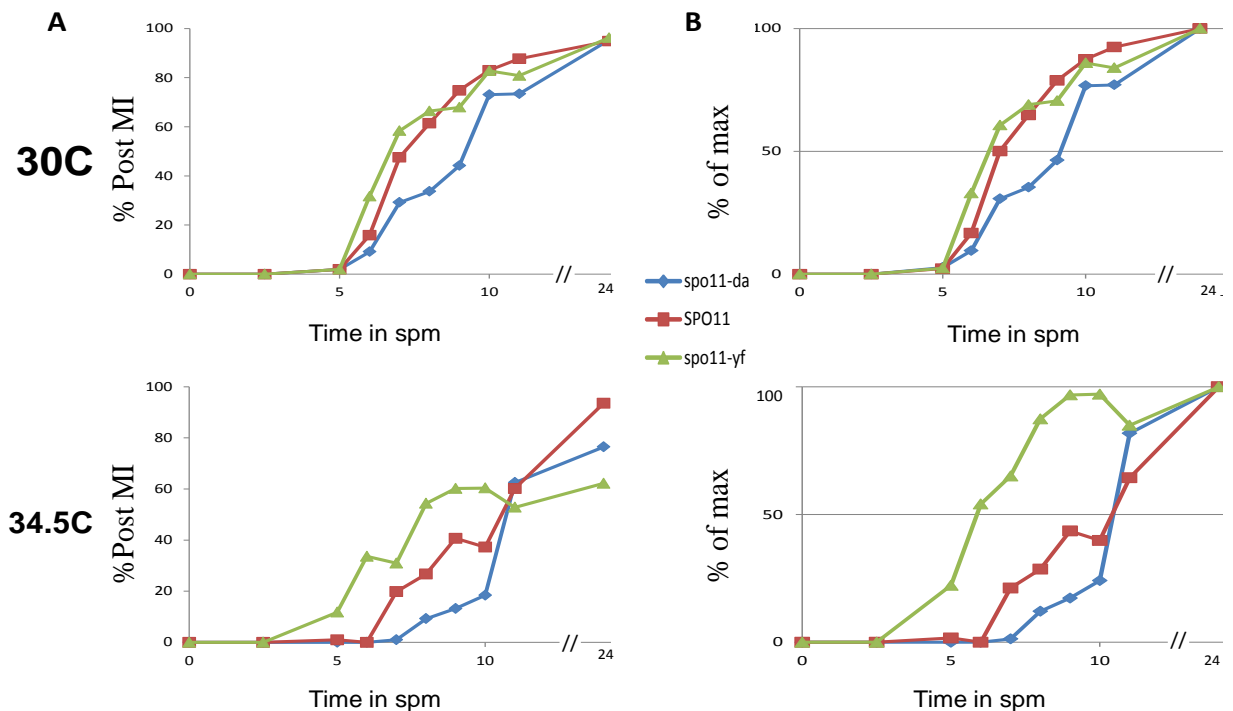
Figure 6. Strains that produce no DSBs progress through meiosis with WT kinetics ofr faster. Meiotic progression in *SPO11*, *spo11-da*, and *spo11-yf* strains. Meiotic progression was monitored by DAPI staining to determine the number of binucleate (MI) and tetranucleate cells (MII). spo11-yf cultures progress through meiosis at WT rate or more expediently while there is a delay in spo11-da cultures at both temperatures. Nuclear divisions were expressed as A. Percent of total cells B. as a percent of maximum.

3.2 Strains that do not form DSBs progress through meiosis with WT kinetics or faster.

My results demonstrate that low double strand break levels delay the occurrence of

the first meiotic nuclear division. My next question was whether elimination of DSBs lead to

either a greater delay, complete meiotic arrest, or no change in nuclear divisions. The *spo11-*

yf strain (SGY 109), which carries a point mutation of the catalytic tyrosine residue to phenylalanine, does not form any DSBs though stable protein is produced and it localizes to chromosomes (Prieler et al.,2005).

I performed multiple experiments in which I compared nuclear divisions in *spo11-yf* cultures to a parallel *SPO11* (VBY 1083) culture. In a representative experiment (TC 12) performed at 30°C, the *SPO11* culture (red) and *spo11-yf* (green) reached the 50% entry mark at 7.0 hours and 6.6 hours, respectively. The *spo11-yf* culture reached the 50% mark slightly earlier than the *SPO11* but this was not observed in all experiments (Fig 6B). The *SPO11* culture reached peak nuclear divisions of 95% and the *spo11-yf* culture reached 96% nuclear divisions for efficiency of ~100% in this experiment (Fig. 6A)

At 34.5°C, the *SPO11* (red) and *spo11-yf* (green) reached the 50% nuclear division mark at 10.5 hours and 5.8 hours, respectively. The *spo11-yf* reached the 50% mark 4.7 hours ahead of the

SPO11 culture (Fig. 6B).

Together, these observations indicate that reduced DSBs trigger an extensive meiotic delay while the absence of DSBs does not. If low DSBs accurately reflect events at an early stage of meiosis, this would indicate that the first DSBs trigger a delay that allows for more time to enhance DSB formation and/or repair. A reasonable inference from this observation is that the response of meiotic cell cycle progression to low DSBs is initially triggered but DSBs quickly accumulate and exceed a threshold level, thus bypassing the delay.

I can also exclude certain alternative explanations. Both *spo11-yf* and *spo11-da* strains exhibit severe SC defects, with the central element protein Zip1 self-associating in large aggregates known as polycomplexes (Henderson and Keeney, 2004). Since both mutants exhibit severe SC defects, it is unlikely that these flaws are responsible for the delay

26

in *spo11-da* cultures.   Finally, I can conclude that the delay

of meiosis in *SPO11* (and *spo11-da*) at higher temperature is caused by a DSB-induced

effect, for which low levels of DSBs are necessary.

3.3 The meiotic delay in *spo11-da* hypomorphs is mediated by the checkpoint component Pch2.

Following the discovery of a delay in meiotic progression at reduced DSBs but not in

the absence of DSBs, I next asked whether the delay at low DSBs (*spo11-da*) is mediated by

a particular checkpoint.   The *Pch2*-mediated checkpoint appeared as an attractive candidate.

Pch2 deletion (*pch2Δ*) bypasses the meiotic arrest in a *dmc1* deletion (*dmc1Δ*) background at

reduced, but not at normal DSB levels (Zanders and Alani, 2011). The Pch2 protein is

thought to monitor residual meiotic DNA damage and/or defects in

SC assembly state. The checkpoint prevents cells from exiting the pachytene stage of

meiosis if these aberrations are present. If the delay I observed is mediated by Pch2, a *pch2Δ*

mutation in a *spo11-da* background would be expected to bypass the delay.

To examine this possibility, I compared meiotic cell cycle progression in isogenic

spo11-da strains defective or WT for *PCH2* in multiple experiments (n=3). Experiments

were all conducted at 30ºC and 34.5ºC. In a representative experiment (TC12), the *spo11-da*

(SGY 148, blue) and the *spo11-da pch2Δ* (SGY 154, purple) reached the 50% entry mark at

9.2 hours and 6.6 hours, respectively (Fig. 7B). This indicates that meiosis I occurs 2.6 hours

earlier when Pch2 is absent in a *spo11-da* background.   Among all experiments considered

(n=3), the mean time difference between the *spo11-da* and *spoll-da pch2Δ* cultures was
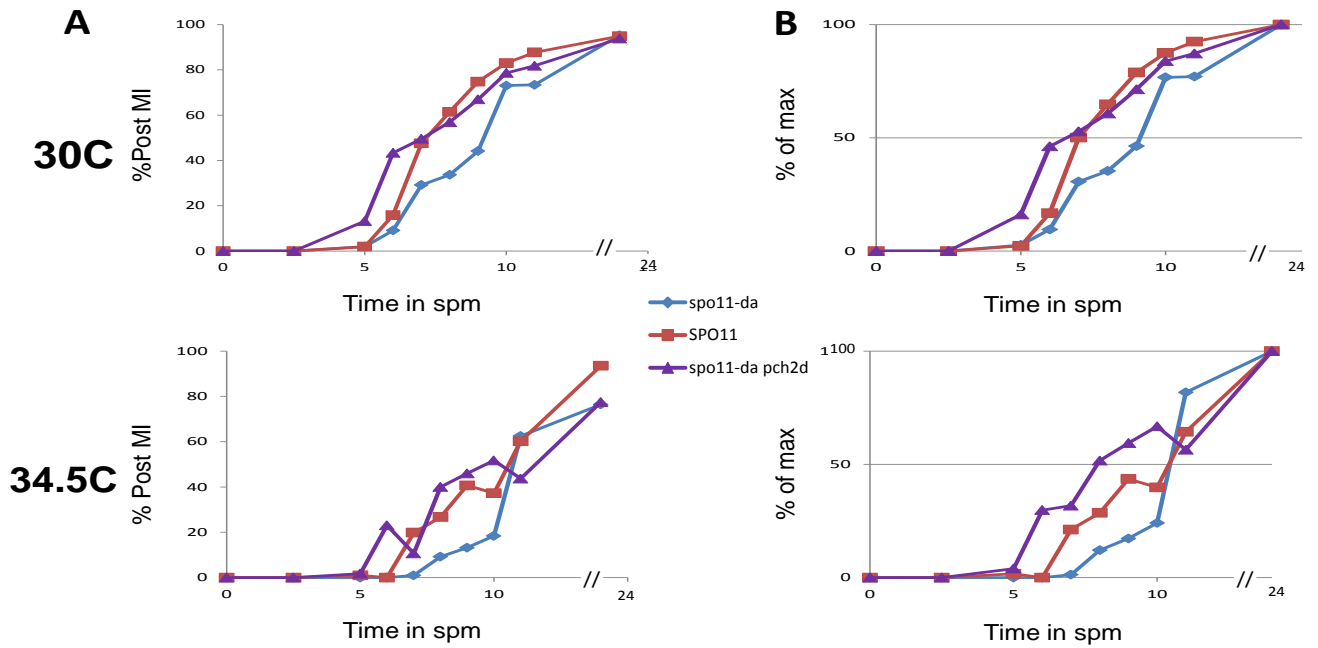
Fig. 7 The checkpoint activated in *spo11-da* mutants is mediated by checkpoint component Pch2. Meiotic progression in *SPO11*, *spo11-da*, and *spo11-da pch2Δ* strains. Meiotic progression was monitored by DAPI staining to determine the number of binucleate (MI) and tetranucleate cells (MII). The pch2d mutantation in a spo11-da background alleviates the delay conferred by the spo11-da mutation alone. Nuclear divisions are similar to the wild type strain at 30C. h temperatures considered. Nuclear divisions were expressed as A. Percent of total cells B. as a percent of maximum

calculated as 1.5 hours +/- .0.39 (mean +/- standard deviations).

Pch2 monitors defects in recombination and/or SC formation and triggers meiotic arrest in the presence of such aberrations. Pch2 further plays an integral role in establishing initial interhomolog bias (Neeraj Joshi and Valentine Borner, personal communications). Taken together with my own data, these findings suggest that Pch2's DSB monitoring function early in meiosis could also trigger the observed delay in meiotic progression in much the same way that it does in the presence of unrepaired recombination intermediates. An alternative explanation is that removal of Pch2 results in inefficient IH bias and DSBs are repaired with the sister chromatid. Since the repair is affected more quickly (Goldfarb and Lichten, 2010), the cell cycle follows in turn. Based on my data, I cannot distinguish between these possibilities.

3.4 The *spo11-da* low spore viability defect is rescued at increased temperature.

Following the discovery that the *spo11-da* mutation confers a transient arrest in meiosis and this arrest was mediated by checkpoint component Pch2, I next wanted to investigate whether the observed delay imparted any growth advantage to the cells. Notably, I assessed spore viability by dissecting tetrads from the same cultures in which meiotic cell cycle progression had been monitored. At 30ºC, spore viability in the *SPO11* strain is between 90 and 100%. In the *spo11-da* strain (blue), the mean spore viability among four cultures was 27% (n=79), consistent with previous reports (19.3%; Diaz et. al, 2002). Surprisingly, the viability for the same cultures that had been shifted to 33.5ºC at the two hour time point increased 2.6 fold to a mean of 69.6% (n=107) (Fig. 8a).

Higher spore viabilities were also observed in homozygous *spo11-da* strains that carried an additional mutation in both yeast loci that encode histone H2A which abrogates
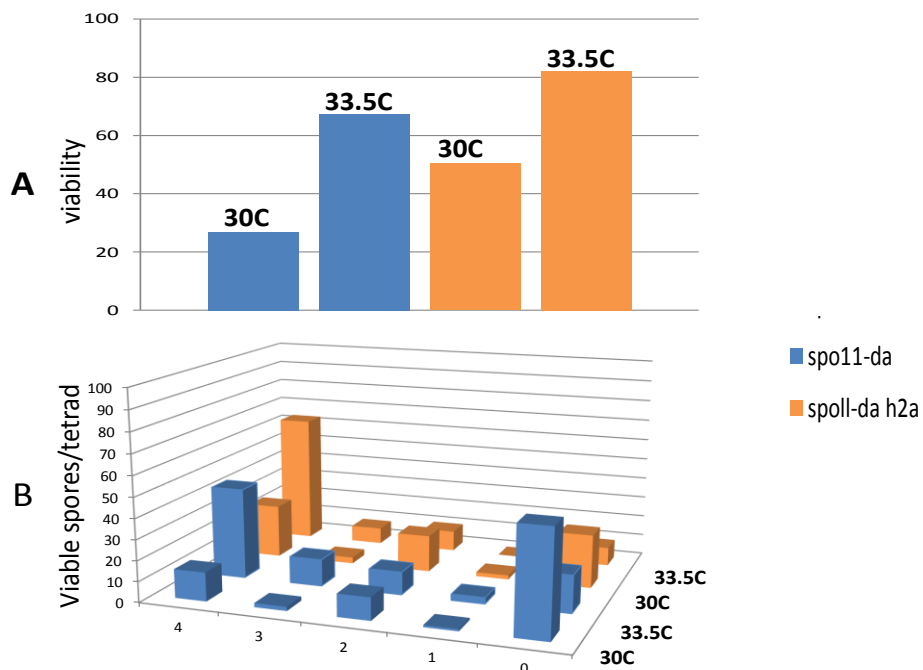
Fig. 8 The low spore viability phenotype conferred by the *spo11-da mutation is rescued at high temperature*
A. Mean spore viabilities of *spo11-da* and *spo11-da h2a* 24 hour cultures at the indicated temperatures among Four experiments. B. Percentage of tetrads with 4, 3, 2, 1, or 0 viable spores per tetrad. Rescue is primarily an increase of 4 viable spore tetrads at the expense of 0 viable spore tetrads.

the phosphorylation site at serine 129 (see below) (*spo11 D290A HA/"*, *h2a S129A/"*

29

hereafter referred to as *spo11-da h2a*). The mean viabilities for *spo11-da h2a* mutants

(orange) among four independent experiments were 40.8% and 82.2% at 30ºC and 33.5ºC,

respectively (Fig. 8a).

When tracking viable spores per dissected tetrad, the increase in spore viability of the

spo11-da hypomorphs at 33.5ºC is primarily due to a rise in four viable spore tetrads at the

expense of zero viable spore tetrads (Fig 8b). This suggests that homolog disjunction is

improved as homolog nondisjunction results in 0 or 2 viable spores. Reasons for this could

include increased COs due to increased DSB levels or increased interhomolog bias.

Nuclear divisions were efficient in *spo11-da* mutants at high temperature and spore

viability was rescued but few tetrads were observable under the tetrad dissection microscope

following zymolyase digestion of spore walls. This may have been simply because there was

a lack of available cells or because asci did not survive digestion. I next asked if the lack of
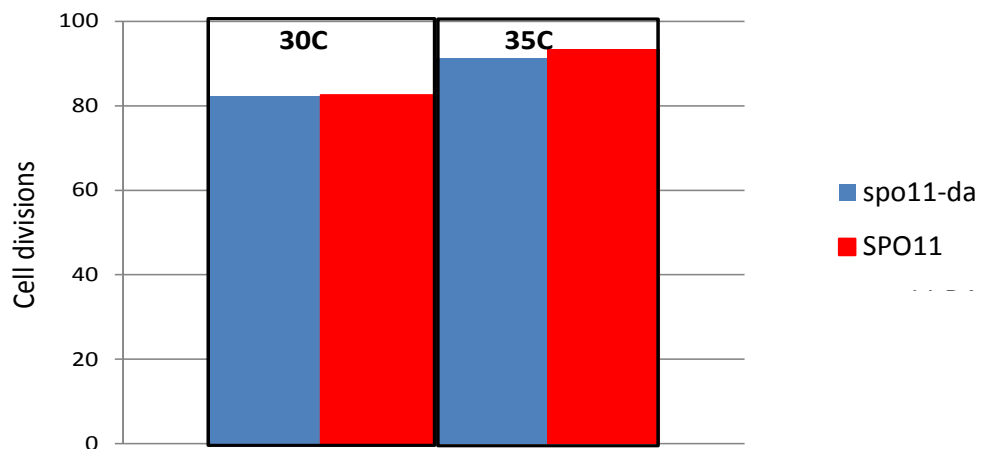
Fig 9. Cell divisions are normal in *spo11-da strains*
at high temperature. Spore formation in *spo11-da* and *SPO11* strains when
sporulated in liquid culture for 24 hours at the indicated temperatures.

observable tetrads was due to inefficient spore formation following nuclear divisions. Spore formation was high in *spo11-da* mutants at high temperature, however; 82% at 30ºC and 91% at 34.5ºC for the *spo11-da* cultures when determined by Nomarski microscopy (Fig. 9). This may indicate that there is a defect in spore wall formation at high temperature and cells did not survive digestion since spore wall integrity is impaired in a microscopically undetectable manner.

3.5 The increased spore viability of *spo11-da* strains at 33.5ºC is not due to an increase in COs

I next asked if the spoll DA strain's increased spore viability at 33.5ºC might be due to increased COs, either due to (A) an increase in DSBs or (B) an increase in IH bias. I monitored CO formation at the well characterized HIS4LEU2 hotspot in *spo11-da* and *SPO11* strains at 30ºC and 33.5ºC, respectively. This hotspot consists of a bacterial sequence that triggers high levels of DSBs integrated at the HIS4 locus together with a LEU2 marker. Two versions of the hotspot, termed "mom" and "dad" have a XhoI restriction pattern dimorphism. Digestion with Xho I produces a restriction fragment of 5.9 kb in the case of the "mom" hotspot and 4.3 kb in the case of the "dad" hotspot. Crossovers at the hotspot produce intermediate length restriction fragments of 5.6 kb and 4.6 kb. These can be visualized on a Southern blot with a radioactive probe specific for the hotspot. The presence of the hotspot allowed me to assess whether increased double strand breaks and/or crossovers occurred at this specific locus in the *spo11-da* culture at 33.5ºC relative to the same culture incubated at 30ºC.

In wild type cultures at both 30ºC and 33.5ºC, DSBs become visible at 3 hours and disappear as they are resolved. COs begin to appear at 5 hours and increase until maximum

31
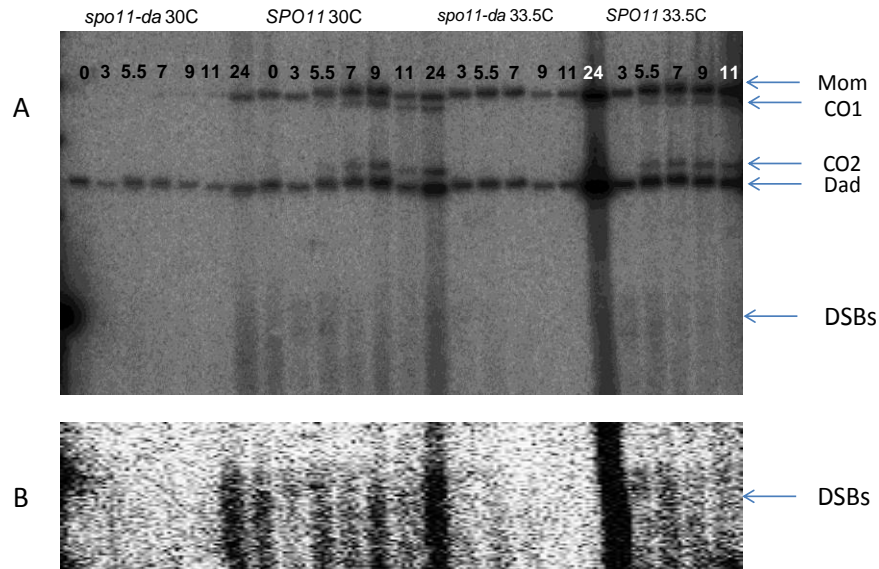
Fig 10 Rescued spore viability in *spo11-da* strains is not due to an increase in COs. CO formation at the HIS4-LEU2 hotspotAt 30C and 33.5C in *spo11-da* and *SPO11* strains. While CO formation is normal in the WT at both temperatures, CO formation is below the level of detection in the spo11-da mutant. A. Southern hybridization of an agarose gel of the meiotic DNA preparations of the strains indicated. B. Darkened image of the lower half of the image shown in A to make the region with DSBs more visible.

levels are reached at 9 hours (Fig.10). In the spo11-da strain at both temperatures DSBs and COs were below detectible levels. This suggests that the increase in spore viability in the *spo11-da* strain at 33.5ºC is not due to an increase in DSB or CO frequencies at the HIS4 LEU2 hotspot. However, since global DSB levels were not measured, this does not rule out the possibility that CO frequencies in other genome regions are increased.

3.6 Increased spore viability in *spo11* hypomorphs is undetectable at higher DSB levels

I next inquired if the rescued spore viability at high temperature is also observable in *spo11* hypomorph strains with higher double strand break levels. Strains with higher DSB levels would be advantageous because an increase in DSBs and COs at 33.5ºC would be detectable by southern blot analysis. I monitored meiotic progression in a diploid strain

heteroallelic for a hemagglutinin (HA) tagged *spo11* allele and a *spo11-da* allele (SGY 151, henceforth referred to as *spo11-ha/da*). This strain produces approximately 50% DSB levels
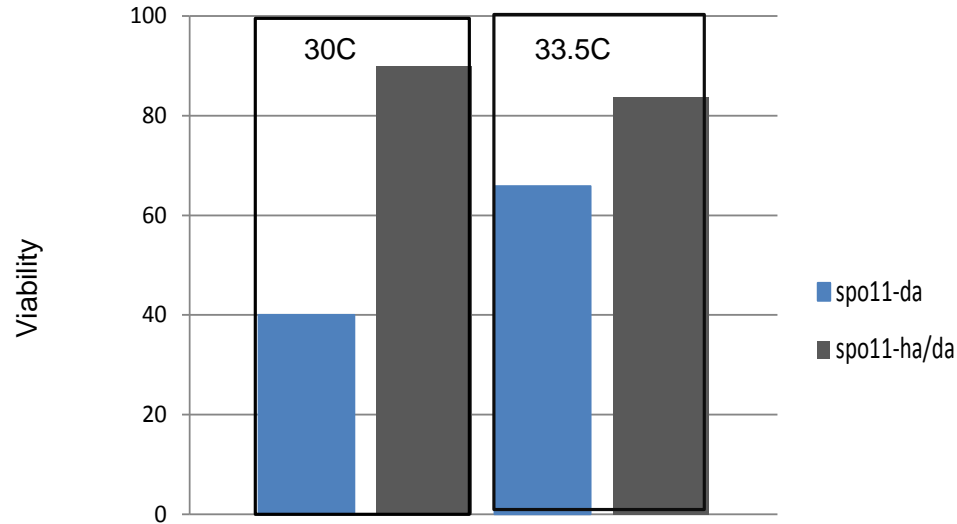
Fig11 Increased spore viability in spo11 hypomorphs is undetectable at higher DSB levels. The increase in spore viability observed in *spo11-da strains (4% -12% of WT DSBs) at* at 33.5C is not recapitulated at higher DSB levels (*spo11-ha/da*, 20% of WT DSBs). Tetrads were dissected of 24 hour cultures of the indicated strains at the indicated temperature. Viability was calculated as a percentage of viable spores out of the total dissected.

relative to *SPO11*. Spore viability in the *spo11-ha/da* strain was 90% at 30ºC and 83.5% at 33.5ºC (Fig. 11). The apparent reduction in spore viability is likely not significant as only a small set of tetrads was dissected under both conditions. Therefore, the rescue of spore viability can only be observed in *spo11-da* hypomorph. This is most likely due to the fact that DSB levels in the *spo11ha/da* are high enough for a single crossover per chromosome to occur, promoting proper chromosome segregation in meiosis I. I therefore reasoned that physical analysis would prove uninformative.

3.7 Phosphorylation of histone H2A is required for normal meiotic progression at all DSB levels.

In male mouse meiosis, the histone H2A variant H2AX is phosphorylated across large

chromosome regions in response to the programmed DSBs that occur in the zygotene stage
of meiotic prophase (Mahadevaiah et. al, 2001). Gamma H2AX foci disappear as DSBs are
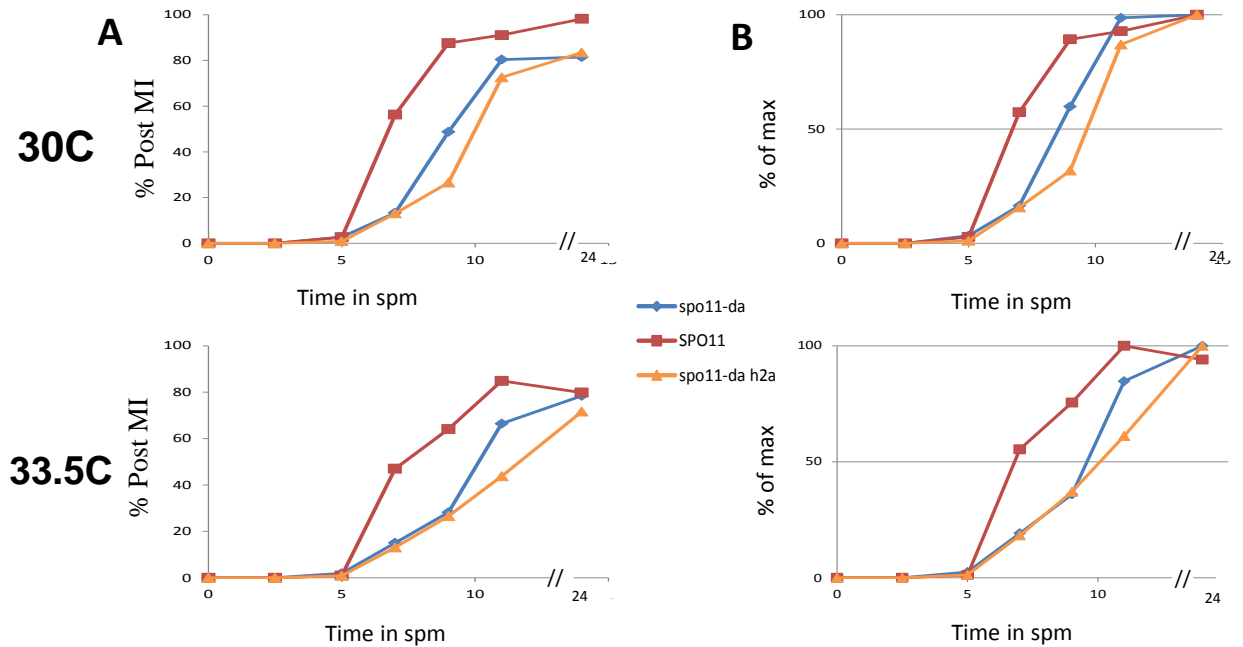
Fig12. The *h2a* mutation confers an additional delay in meiotic progressions in the *spo11-da* background.
Meiotic progression in *SPO11*, spo11-da, and *spo11-da h2a* strains. Meiotic progression was monitored by
DAPI staining to determine the number of binucleate (MI) and tetranucleate cells (MII) then graphed as a
percentage of total cells. Nuclear divisions are delayed in spo11-da h2a strains relative to both the spo11-da
and SPO11 strains at both temperatures considered. Nuclear divisions were expressed as A. Percent of total
cells B. as a percent of maximum

repaired and a second round of H2AX phosphorylation occurs in the unsynapsed regions of

the XY pair of sex chromosomes (Fernandez-Capetillo et al.,2003). While function of H2AX

has been investigated in the mouse model , no role has been established in yeast meiosis

(Michael Lichten, personal communication).

Yeast H2A has been implicated in DNA damage checkpoint function in yeast mitosis

and absence of Tel1/ATM results in reduced spore viability, specifically at low DSB levels. I

therefore asked if the checkpoint triggered in spo11-da strains might be mediated by H2A

phosphorylation in addition to Pch2 or along the same pathway as Pch2. To address this

question, I monitored meiotic progression in a a *spo11-da* (Blue), a *spo11-da h2a* double

mutant (SGY 149, orange), and a *SPO11* strain (VBY 1083, red). The experiment was performed at 30ºC and 33.5ºC, beginning with a single culture of each strain and splitting them at the two hour time point to ensure efficient progression through S-phase. Half of the initial culture was placed at 30ºC and half at 33.5ºC, respectively. Both cultures were incubated for the remainder of meiosis at their respective temperatures.

In contrast to my expectations, the *spo11-da h2a* culture exhibited an additional delay relative to the *spo11-da* strain at both temperatures. Specifically, at 30ºC, the *spo11-da h2a* strain was 1 hour delayed relative to the *spo11-da* strain and 2.8 hours delayed relative to the parallel *SPO11 H2A* strain. At 33.5ºC, the *spo11-da h2a* strain was 0.6 hours delayed relative to the *spo11-da* strain and 3.8 hours delayed relative to the parallel *SPO11 H2A* strain (Fig 12b).

Since the *h2a-s129a* mutation confers an additional delay to the *spo11-da* strain background, it is questionable whether the DNA damage checkpoint is compromised due to the absence of H2A phosphorylation. However, it may implicate H2A phosphorylation in timely DSB repair during meiosis or some other meiotic process (see discussion). The additive effect of the *spo11-da* and *h2a* mutations suggests that the mechanism of each delay is distinct and separate. It also suggests that checkpoint function in yeast is not abrogated in *h2a* mutants, which is surprising, since H2AX phosphorylation is intimately tied to DNA damage checkpoint function in mammals (see introduction).

I next asked whether the additional delay in nuclear divisions of the *spo11-da h2a* mutant relative to *spo11-da* strain was peculiar to reduced DSB levels (*spo11-da*) or if it was also observable in strains with higher DSB levels. To test the hypothesis that the *h2a* mutation confers a delay in meiotic progression at all DSB levels, I introduced mutant alleles hta1-S129A and hta2 s129a into both the SPO11 and the heterozygous *spo11-ha/da*

backgrounds. Since mutant alleles are unmarked, they were followed by restriction

polymorphism during strain construction (Materials and Methods). Meiotic progression was
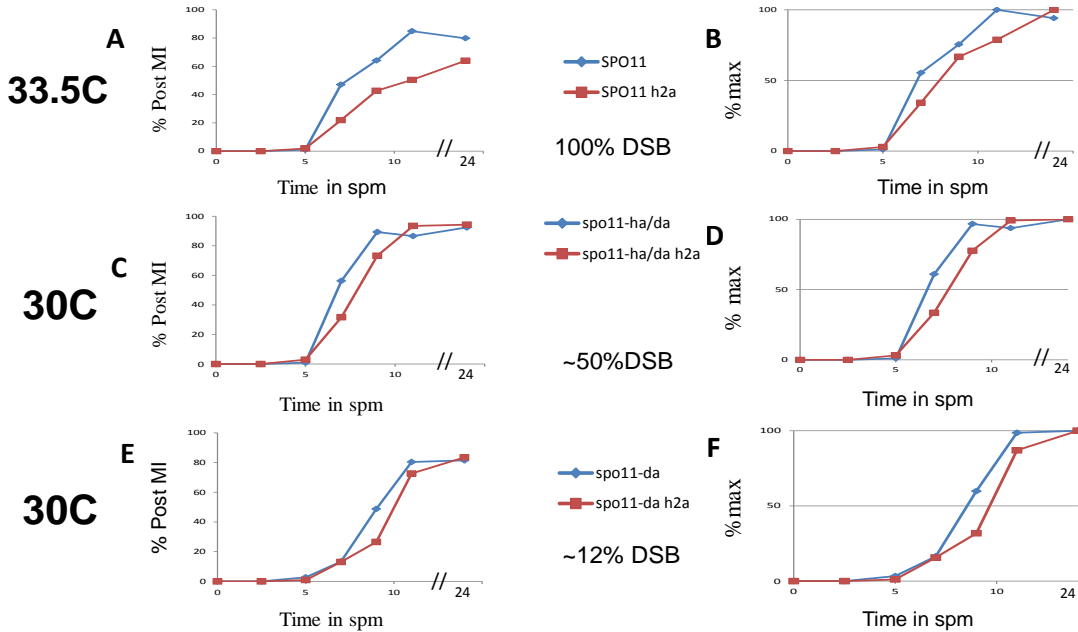
Fig. 13 The h2a mutation in a *spo11* hypomorph background confers a delay in nuclear division relative to spo11 hypomorph single mutants at all DSB levels. Meiotic progression was monitored by DAPI staining to determine the number of binucleate (MI) and tetranucleate cells (MII). A. *SPO11 h2a* exhibited a delay in nuclear divisions relative to SPO11 In liquid culture at 30°C C) , *spo11-ha/da h2a* exhibits a delay in nuclear divisions relative to *spo11-ha/da* In liquid culture at 30°C, E) *spo11-da h2a* exhibits a delay in nuclear divisions relative to *spo11-da* In liquid culture at 30°C. B, D, and F. Same as a-c normalized for 50% max

monitored in the strains carrying the *h2a* mutation relative to the isogenic *H2A* wild type

strain. These were: a *spo11-ha/da* strain (SGY 151, blue, 50% WT DSB levels), a

corresponding *spo11-ha/da h2a* (SGY 150, red) strain, a *SPO11* strain (VBY 1083, blue), and

a *SPO11 h2a* strain (SGY153, red). At the 2 hour time point, I split the cultures into two

temperatures, 30ºC and 33.5ºC, and incubated for the remainder of the experiment.

At 30ºC, there was no delay in a *SPO11 h2a* single mutant strain relative to the

SPO11 strain (data not shown). At 33.5ºC, however, the *SPO11 h2a* strain exhibited a 1.2

hour delay relative to the *SPO11 H2A* culture (Fig. 13a and 13b). The *spo11-ha/da* h2a strain

displayed a 1.2 hour delay relative to the *spo11-ha/da* strain (Fig. 13c and 13d).

Since there is an additive effect of reduced DSB and *h2a* mutation in the *spo11-da*

36

h2a mutant, I conclude that the each mutation contributes independently to the delay. As a delay was observed at all DSB levels this suggests that the delay observed in *spo11-da*
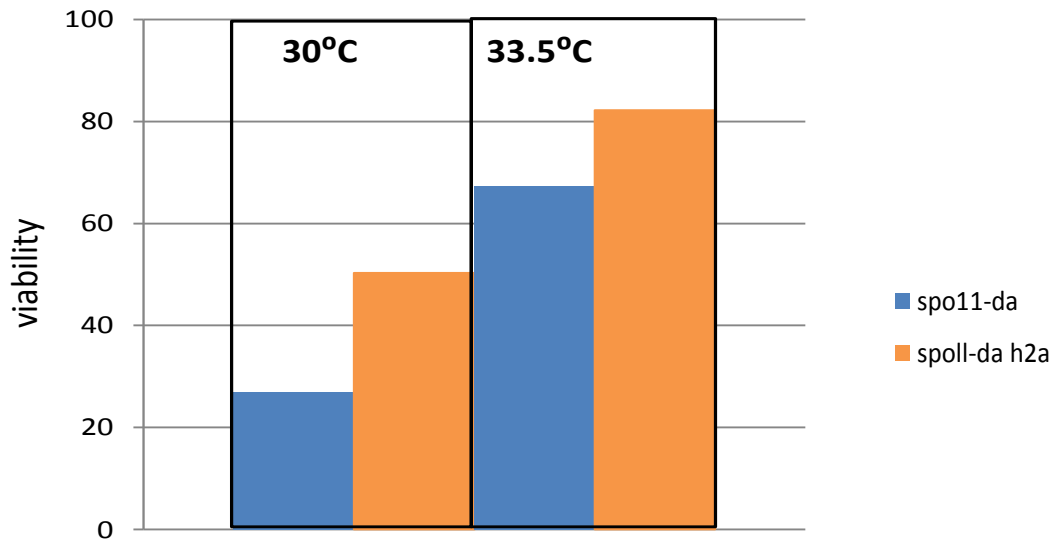
Fig. 14. The h2a mutation confers an increase in spore viability in the spo11-da background Spore viability of *spo11-da* and spo11-da h2a cultures at 33.5^{o}C. Tetrads were dissected of both *spoll–da* and *spo11-da h2a* cultures that had been incubated at the indicated temperatures for 24 hours. The number of viable spores was calculated as a percentage of the total spores dissected

cultures and that conferred by the *h2a* mutation function through separate pathways. Possible explanations are (i) that a second checkpoint has been activated, (ii) that repair proteins aren't properly recruited to the site of DSBs and it takes more time for repair to be completed, or (iii) that repair with the sister chromatid (IS repair) is abrogated and repair is directed toward the homolog, which requires more time than IS repair. The viability data presented below supports the last possibility.

3.8 The *h2a* non-phosphorylatable mutation confers an increase in spore viability at two DSB levels.

Rather than eliminating delay as I expected, I found that the *h2a* S129A mutation extends the duration of the meiotic progression delay. This delay may indicate an additional

activated checkpoint, a more severe defect, or both. As checkpoints are activated to provide additional time for cells to accomplish certain tasks, avoiding catastrophic consequences (e.g. to repair DNA damage), I next asked what advantage the additional delay might impart the cells. To that end, spore viabilities at all DSB levels were monitored.

The most striking effect was apparent in *spoll-da* vs *spo11-da h2a* strains when averaged among four independent experiments (Fig. 14). At 30ºC the *spo11-da* strain demonstrated an average spore viability of 26.9%. The *spo11-da h2a* strain, on the other hand exhibited nearly twofold increase in

spore viability to 50%. At 33.5ºC the trend persisted; average viability for the DA strain was 67.3%.

whereas Spo11-ha/da h2a strain at 33.5ºC was 82.2% viable. One attractive interpretation of these findings is that the delay conferred by the h2a mutation grants a viability advantage to the cells.

H2a mutants in all *SPO11* backgrounds showed an increase in overall spore viability at 30ºC, increasing from 40% to 45% in the case of *spo11-da* vs. *spo11-da h2a* cultures (Fig. 15). In *spo11-ha/da* vs *spo11-ha/da h2a* cultures at 30ºC, the increase was from 90% to 96.5% (Fig. 15). The rise was from 90.5% to 100% in the case of *SPO11* vs *SPO11 h2a* strains. For the *spo11-da* hypomorphs, the trend was even more pronounced at 33.5ºC. The *spo11-da* single mutant showed 65.8% viability while the spo11-da h2a strain exhibited 91.5% spore viability (Fig. 15). The *spoll-ha/da* vs *spo11-ha/da h2a* strain also had a more pronounced difference compared to the corresponding 30ºC culture (83.8% spore viability vs. 93.1%, respectively), although the overall spore viabilities were decreased. The only exception to the trend was *SPO11* at 33.5ºC which exhibited 100% viability though the *SPO11 h2a* mutant displayed only 95% viability; this may have been due to normal variation

in viability, however, and unrelated to the difference in temperature.
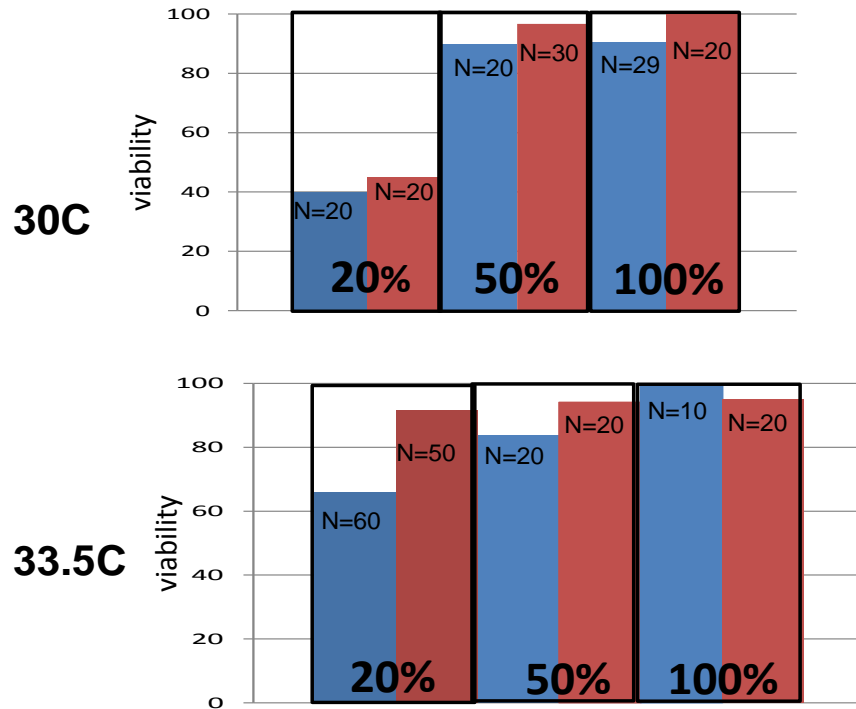
Fig.15 h2a mutation confers an increase in spore viability at two DSB levels at two temperatures considered. DSB levels for each SPO11 allele is shown at the base of the bar graphs. The number of tetrads dissected is shown at the top of each bar.

3.9 Establishment of a genetic screen to identify genes that genetically interact with PCH2 and SPO11.

At the start of this project, little was known about why absence of Pch2 reduces spore viability at low DSBs. To elucidate Pch2's role in yeast meiosis, I performed a multicopy suppressor screen. Multicopy suppressor screens are based upon the concept that, if a gene is mutated, overexpression of a genetically related gene may partially or completely rescue the displayed mutant phenotype.

An overexpressed gene can rescue a mutant phenotype via three possible mechanisms. First, the overexpressed gene could produce a protein that participates in a

complex with the mutated protein. Often this partially compensates for the mutation. Second, it could be a protein that lies downstream in a pathway in which the mutated gene participates. In this case, overexpression may bypass the upstream events in the disrupted pathway. Third, the overexpressed gene could code for a protein that participates in a pathway that lies parallel to that of the gene in question. In this situation, both pathways have the

same end result; overexpression increases the output of the parallel pathway, thus compensating for the disrupted pathway's lack of activity (Apping, 1999).

I employed a multicopy genomic library in which random fragments of the yeast genome are ligated into the 2 micron shuttle vector yEP13 (Nasmyth, 1980) (henceforth referred to as the Nasmyth library). yEP13 is a shuttle vector and can be stably transmitted in both E. Coli and Yeast. It contains an ampicillin gene for selection in E. coli and a LEU2 gene that complements auxotrophy in S. Cerevisiae.

Initially, I did not know what DSB level or temperature conditions would be optimal for the screen and I performed a pilot experiments with two pairs of *spo11* hypomorphs in the presence and absence of the *pch2Δ* mutation. In the pilot experiment, a *spo11-ha/yf* heterozygous strain (SGY13) was paired with a *spo11 ha/yf pch2Δ* (SGY14; ~30% of *SPO11* DSBs), and a *spo11-da* strain (SGY15 ~20% of *SPO11* DSBs) was paired with a *spo11-da pch2Δ* double mutant (SGY16). Each of these were heterozygous for cycloheximide resistance. Cyclohiximide sensitivity is dominant over reisitance, which provided a means to select against unsporulated heterozygous diploid cells. Therefore, only cells that had completed sporulation and received a copy of the cycloheximide resistance gene grew, while unsporulated diploids remained cycloheximide sensitive.

All four strains were inoculated in triplicate in a 96 well microtiter dish in liquid

media lacking arginine (arg-) and were allowed to grow to saturation at room temperature. Cells were resuspended and stamped with a frogger to rich sporulation media (spmr), which allows growth into a visible cell patch followed by growth arrest, entry into meiosis, and spore formation. The cells were allowed to sporulate at three temperatures (23°C, 30°C, and 33°C). Spmr plates were replica plated to arg- media supplemented with cycloheximide. The arg- cyc plates were incubated at three temperatures (23°C, 30°C, and 33°C) until there was visible growth. No growth was observed in the *spo11-da pch2Δ* or *spo11-ha/yf pch2Δ* strains whereas the *spo11-ha/yf* and *spo11-da* single mutants showed significant growth as clusters of microcolonies. Since there was a clear growth difference between the *spo11-da* hypomorph and its respective pch2 deletion counterpart at 30°C (figure16), all further experiments were carried out with *spo11-da* and *spo11-da pch2Δ* strains at 30°C.

The Nasmyth library was marked with a WT LEU2 gene so it was necessary to construct a *spo11-da pch2Δ* strain with a leu2 auxotrophy (leu-). SGY53 was mated to SGY96 to produce SGY98, a *spo11-da pch2Δ* leu- diploid that was suitable for transformation with Nasmyth library plasmids.

To ensure that the low spore viability phenotype of a *spo11-da pch2Δ* strain could be complimented, I performed a mating of a *spo11-da pch2Δ* strain and a *SPO11 pch2Δ* strain. The viability of the heterozygous *spo11-da/SPO11 pch2Δ* and *spo11-da pch2Δ* strains were 86.4% and 1%, respectively, indicating that a single genomic copy of the *SPO11* gene

Strain	% spore viability
SGY 98 transformed with PVB30	1%
SGY 98 transformed with S4A	78.3%
SGY 48 transformed with pVB 30	32.6%

Table I. Spore viability of screen controls

complements the *spo11-da pch2Δ* phenotype. Since a single copy of *SPO11* rescued spore

viability, a plasmid with a WT copy of *SPO11* was constructed (plasmid S4A, see Materials

and Methods). The *spo11-da pch2Δ* (henceforth test strain) was transformed with S4A and its

spore viability was found to be 78.3% (Table I), demonstrating that the low spore viability

phenotype had been complemented by an exogenous copy of *SPO11*. The test strain

transformed with S4A was used as a positive control in the screen.
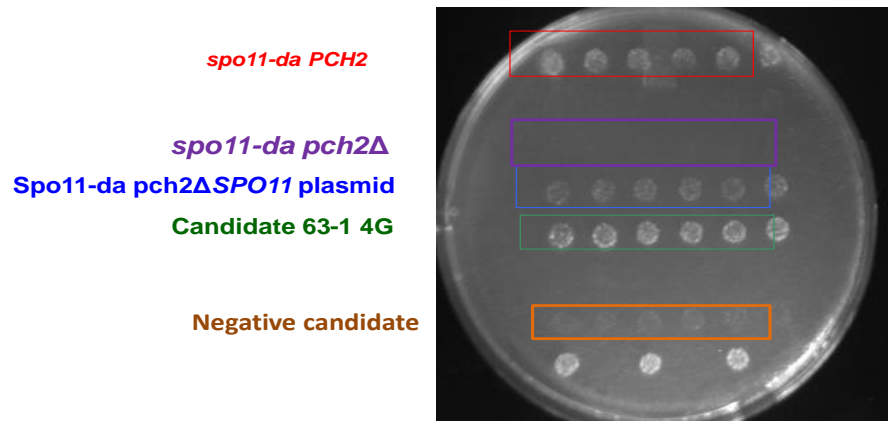
Fig. 16 HS plate of candidates and controls of the indicated genotypes. Candidates were genotype *spo11-da pch2Δ* transformed with library plasmids. Cells were allowed to sporulate on spmr leu- then replica plated to HS media and incubated until there was Significant observable growth. Candidate 63-1 4G was identified as a *SPO11* containing plasmid

Since the *spo11-da PCH2* strain visibly grew on leu- plates supplemented with

cycloheximide (haploid selection, or HS media), I used a strain of this genotype (SGY 48) as

a second positive control. The spo11-da PCH2 strain exhibited a spore viability of 30%.

This demonstrated complementation of the low spore viability phenotype via genomic *PCH2*

WT allele. Since this strain carried an auxotrophy for leu2, it was transformed with pVB30,

an ARS CEN plasmid that is marked with LEU2 and carries a nonfunctional copy of *zip*1, a

component of the SC. PVB30 transformed SGY48 exhibited spore viability similar to that of

42

untransformed *spo11-da* single mutants and was used as a second positive control in the screen. When transformed with pVB 30, the test strain exhibited spore viability congruent with untransformed *spo11-da pch2Δ* (1% spore viability) so it was used as a negative control.

Transformants were derived from a single colony which contained a single plasmid. Transformants and controls were inoculated into leu- liquid media in 96 well microtiter dishes. These were grown to saturation and stamped to supplemented sporulation medium (spmr leu-), which had been optimized for the screen (see Materials and Methods) in addition to leu- backup plates. Following sporulation, the spmr leu- plates were replica plated to HS mediaCandidates exhibited high spore viability (clusters of many microcolonies) whereas cells that were not rescued presented low spore viability (Fig. 16).

Initial candidates were identified and then clone colonies derived from the original transformant were taken through the process outlined above in triplicate. Candidates that produced visible cell patches in triplicate on HS media were accepted as a secondary candidate. Retesting in triplicate more stringently controlled for the possibility that local conditions on the haploid selection media had imparted a growth advantage to the candidate.

While growth on HS media plates afforded a gross readout of candidates' spore viability, once a candidate had retested positively, a more accurate measurement was necessary. To that end, tetrads derived from each candidate were dissected on solid YPD media (N=20 tetrads) and spore viability was assessed. Candidates that exhibited higher spore viability than a *spo11-da pch2Δ* negative control were accepted as final candidates.

To recover the shuttle plasmids containing the presumed suppressor genes from yeast, I used the Yeast High Efficiency plasmid rescue protocol (see Materials and Methods). The plasmids were amplified in bacteria and plasmid extractions were performed to isolate them. Plasmid extracts were digested with EcoRV, which produced characteristic yEP13 backbone

fragments of 3.2 kb and 920 bp and variable fragments of the genomic insert (Fig. 17). No two candidate plasmids exhibited the same restriction pattern. Plasmids were sequenced with the Sanger method.
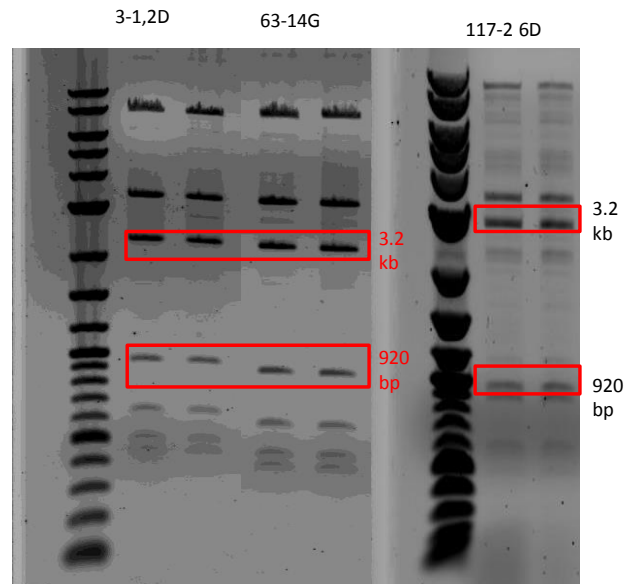
Fig. 17 Eco RV digestions of candidate plasmids. Plasmid DNA extractions were performed on DH5α cells containing candidate plasmids. Plasmid preps were digested with Eco RV and loaded In a 0.7% agarose gel then run at 135 volts until DNA was resolved. Highlighted bands are 3.2 Kb and 920 bp which are characteristic of the Yep13 plasmid backbone.

3.10 Overexpression of Hop1 axis protein suppresses chromosome segregation defects in *spo11-da pch2Δ*.

14,400 transformants were screened which gave rise to 79 primary candidates, 25 secondary candidates, and 7 final candidates (Table II) of which three have been sequenced and identified. One (candidate 117-2 6A) is a plasmid containing the genes HOP1, PCI8, and MAM33 and the other two are *SPO11* containing plasmids (candidates 3-1 2D and 63-1 4G). Extracted plasmids were retransformed into the test strain and tested in triplicate, followed by tetrad dissections. Both *SPO11* containing plasmids and candidate 117-2 6A

44

rescued the low spore viability phenotype when reinserted into yeast.

Recently, low spore viability in a *pch2Δ rad17Δ* was shown to be suppressed by a constitutively active Mek1 effector kinase. Mek1 functions downsteam of Hop1 and plays an integral role in establishing interhomolog bias so I initially believed this to be the mechanism of rescue in candidate 117-2 6A. However, since Hop1 plays a dual role in both the formation of normal levels of DSBs and in establishing IH bias, I could not be sure which activity conferred the rescue of the low spore viability phenotype; it could genetically interact with either Spo11 or pch2. Therefore, future experimentation must be conducted. A table listing 25 secondary candidates follows.

candidate   Viable spore tetrads

plate	well	4	3	2	1	0	% viable
3--1	2D	12	1	3	4	0	76%
15--2,	6A	0	0	7	4	2	45%
15--2,	6C	0	0	0	0	10	0
16--1	2A	0	0	1	3	6	13%
17--1,	2D	0	0	3	0	17	8%
17-1,	3A	0	0	4	4	12	15%
17-1	4D	0	0	3	3	14	11%
30-2,	2B	0	0	8	1	1	43%
36-2,	6E	1	0	0	0	9	10%
40-1,	2B	0	0	10	0	0	50%
43-2,	2H	0	0	0	2	8	5%
63-1,	4G	7	2	0	0	1	85%
71-1,	6C	8	0	2	0	0	90%
87-1,	6E	0	0	0	1	9	3%
117-2	4D	6	3	0	0	1	83%
125-1	6D	0	0	1	1	8	8%
131-2	2D	0	0	1	3	6	13%
132-1	6E	0	1	0	0	9	8%
149-1	6G	9	0	0	0	1	90%
153-1	1H	8	0	1	0	1	85%
183-2	5D	n.d					n.d.
185-2	5H	n.d					n.d
195-2	3A	n.d					n.d.
196-2	4G	n.d					n.d.

Table II. Secondary and final candidates and their spore viabilities

CHAPTER IV

DISCUSSION

4.1 Low DSB levels trigger a novel, DSB-sensitive meiotic checkpoint

Prevailing models depict checkpoints as having evolved to prevent cell cycle progression in presence of aberrant events thus preventing cellular catastrophe. Delayed/arrested cell cycle progression in turn allows additional time for correction of triggering defects. The (mitotic) DNA damage checkpoint, for example, detects the presence of DNA damage during S and/or G2 phase and prevents cell division to allow additional time for DNA damage repair. Checkpoint function was elegantly illuminated in a series of experiments performed with a yeast *rad9* mutant strain (Hartwell and Weinert, 1988). In *rad9*, DNA damage checkpoint function is abrogated. When irradiated, *rad9* mutant strains are viable for several generations but then cease to divide. Thus, *rad9* cells are hypersensitive to DNA damaging agents such as ionizing radiation. When the cell cycle was artificially extended by intermittent exposure to spindle poison following IR exposure, *rad9* cell viability was restored (Weinert and Hartwell, 1988).

During WT meiosis, initiation of recombination delays onset of the first meiotic division: Deletion of recombination initiation genes (e.g. *SPO11* or *MER2*) results in an earlier onset of the first nuclear division, suggesting that recombination initiation, but not

46

absence of DSBs, triggers a meiotic delay (Malone et al., 2004). I observed that nuclear

divisions in *spo11-yf* occur with WT timing at 30°C, but >3hr earlier than in *SPO11* at 34.5°C,

lending support to these reports (Figure 6). Results presented here indicate that low DSB

levels trigger a more extended delay compared to full DSB levels (Figure 6). Together, these

findings suggest that absence of DSBs fails to trigger a checkpoint, but low (i.e. insufficient)

levels of DSBs do trigger a meiotic delay. This delay is checkpoint-mediated (below). I

propose to consider the permanent low DSB levels analyzed here (*spo11-da*; Henderson and

Keeney, 2004) as a model for a transient stage during WT meiosis, when the first DSBs arise.

This suggests that a checkpoint is in effect under the conditions of early meiosis to prevent

meiotic progression before DSBs have reached a minimum threshold. Whether DSBs or

some other signal triggers this transient arrest is not addressed by these observations. By

implication, a DSB-activated checkpoint controls meiotic progression not only when

recombination intermediates are not processed properly, but also during WT meiosis.

4.2 The checkpoint monitors insufficient DSBs, but not defective SC formation

While meiotic events other than DSBs could be responsible for triggering the delay in

the *spo11-da* hypomorph, it is more likely that low levels of DSBs trigger the observed delay.

To address this question further, I monitored nuclear divisions in a catalytically inactive

spo11 null mutant. In *spo11-yf,* no DSBs are produced and severe SC defects are apparent

(Henderson and Keeney, 2004). The SC central element protein Zip1 does not associate with

the axial elements but instead forms self-associated aggregates known as polycomplexes.

If the checkpoint monitors is SC defects, a delay should also be evident in a *spo11-yf*

hypomorph (no DSBs). If the checkpoint is triggered by low DSBs, on the other hand, then it

stands to reason that a lack of DSBs would trigger an even more marked delay. Surprisingly,

I found that the catalytically inactive spo11 mutant progresses through meiosis with wild type kinetics or faster. Since there are even more severe SC defects in the absence of DSBs than at low DSB levels, it is unlikely that abnormal SC formation is the triggering defect. Instead, my results indicate that there is a checkpoint in which low levels of DSBs are recognized as a defect, but surprisingly, this checkpoint is not activated by the lack of DSBs. I propose that a checkpoint transiently arrests the meiotic cell cycle, presumably to allow more time for DSBs to accumulate and allow crossover formation and hence homolog segregation. This checkpoint might monitor recombination-associated components and/or recombination intermediates themselves. The arrest signal could be silenced as soon as a critical, possibly CO-specific intermediate has formed. Without DSBs (*spo11-yf*), the checkpoint machinery may never be put in place, and therefore cannot trigger a delay. At full DSB levels (*SPO11*), the checkpoint requirements may be met more expediently due to rapid accumulation of the silencing signal (above).

4.3 Pch2-mediated checkpoint activity at reduced DSB levels: possible mechanisms

I have uncovered a checkpoint which is activated by low levels of DSBs but not a lack thereof. I next wanted to identify the pathway by which this checkpoint operates. The checkpoint protein Pch2 is part of a checkpoint that monitors recombination intermediates and/or SC assembly in the pachytene stage of meiosis I (San-Segundo and Roeder, 1999; Wu and Burgess, 2006). When Pch2 is absent at low DSB levels, I found that cells return to WT meiotic kinetics, suggesting that Pch2 mediates the checkpoint activity specifically at reduced DSB levels (Figure 7). Interestingly, absence of Pch2 at normal DSB levels results in a marked delay in meiotic cell cycle progression (Wu and Burgess, 2006; Börner et al., 2008). However, the delay observed at WT DSB levels is likely due to Pch2's role in DHJ

resolution rather than in the checkpoint I observed (Börner et al., 2008).

Pch2 has been implicated in such diverse activities as influencing partner choice in meiotic recombination (Ho and Burgess, 2011), chromosome axis morphology (Joshi et al.,2009), and preventing recombination adjacent to nucleolar rDNA repeats (Vader et al., 2011) in addition to mediating the pachytene checkpoint. Little is known about its mechanism of activity. The pachytene checkpoint is thought to be triggered by defects in recombination and/or SC formation. It is likely that one of these stimuli evoked the checkpoint activity I observed. An important question to answer, therefore, is which defect triggers the Pch2-mediated checkpoint.

In the budding yeast *S. cerevisiae*, accumulated resected DSBs due to *DMC1* deletion cause a Rad17 dependent arrest in the meiotic cell cycle (Ho and Burgess, 2011). In some studies, Pch2 was also found to mediate this arrest, potentially only at reduced DSB levels (San-Segundo and Roeder 1999; Zanders and Alani, 2011). In both *D. melanogaster* and C. *elegans,* on the other hand, Pch2 checkpoint function does not appear to monitor DSB processing at all. In both organisms and in contrast to yeast, synapsis and meiosis proceed normally even in the absence of DSBs. In *D. melanogaster* and *C. elegans*, a Pch2 dependent checkpoint is activated when defects in chromosome synapsis are introduced (Bhalla and Dernberg, 2005; Joyce and McKim, 2008). Similarly, in the case of a *zip1Δ* mutant in *S. cerevisiae*, a synapsis-dependent checkpoint that is mediated by Pch2 is triggered (San-Segundo and Roeder, 1999). In a *spo11-da* mutant in yeast, proper synapsis may not be established as evidenced by the lack of full SC formation (Henderson and Keeney, 2004). However, since SC formation is abrogated when no meiotic DSBs are present, SC defects are unlikely to be the triggering defect for the PCh2-mediated checkpoint in *S. cerevisiae*.

49

Further experimentation is required to dissect the checkpoint function. One way of doing this might be to construct a *spo11-da* double mutant in which interhomolog bias is not properly established. For example, a non-phosphorylatable allele of *HOP1* or a loss of function mutation in Mek1 would preclude the establishment of interhomolog bias, allowing the efficient repair of DSBs with the sister chromatid (Niu et al.,2009; Carballo et. al, 2008). If improper synapsis is the cause of the delay I observed, it would still be evident in such a mutant. However, as no evidence has yet been presented regarding SC assembly when IH bias is deficient, it would be necessary to view Zip1 polymerization to demonstrate more conclusive proof.

Another line of questioning involves the mitotic checkpoint protein Rad17. Rad17 mediates a checkpoint pathway that is parallel and partially redundant with the function of Pch2 (Ho and Burgess, 2011). Therefore it would also be interesting to monitor meiotic progression in a *spo11-da rad17Δ* mutant and compare the effect on meiotic progression with that of *spo11-da pch2Δ*. I expect that deletion of the checkpoint protein in the presence of low DSBs would reduce spore viability to levels similar to that of *spo11-da pch2Δ*.

4.4 Meiotic defects at low DSB levels are rescued by higher temperatures.

At low DSB levels, a process known as CO homeostasis increases COs at the expense of NCO events (Martini et al., 2006). A *spo11* hypomorph that produces only 50% of WT DSBs, for example exhibits WT spore viability since at least one CO per chromosome appears to form and meiotic chromosome segregation proceeds normally. When CO are reduced below a threshold level, spore viability is reduced in response. My results demonstrate that a *spo11-da* hypomorph, which produces 4-20% DSBs, exhibits a spore viability of ~27% at 30ºC. Though the delay in nuclear divisions is still apparent at 33.5°C,

spore viability is significantly greater at this temperature compared to 30°C.

There are several possible reasons for the increased viability in *spo11-da* cultures at 33.5ºC. First, higher temperature may enhance the activity of Spo11-da, resulting in increased DSBs and hence CO levels. Notably, several *spo11* hypomorphs are intrinsically cold-sensitive (Diaz et al., 2002). I addressed this issue by measuring DSBs at the *HIS4LEU2* hotspot. DSBs and COs at this hotspot were below the level of detection, suggesting that the improved spore viability was not due to an increase in DSB levels at this specific locus (Figure 10). While DSB measurement at *HIS4LEU2* is a useful tool, it cannot be excluded that global DSBs were increased to the point where spore viability was rescued.

A second possibility is that the formation of the SC, which mediates DSB repair with the homologue, may have been rescued in *spo11-da* cultures at 33.5ºC. Mutants defective in SC formation such as *zipΔ* form CO at reduced levels and these appear at a later time than WT strains (Storlazzi et al.,1996). A restoration of the SC might also restore the efficiency of DSB repair with the homolog leading to CO. Alternatively, IH bias may be increased at high temperature. In this case, a barrier to IS repair would be established such that repair with the homolog would be increased at the expense of IS recombination (Schwacha and Kleckner, 1997). However, as no detectable CO were observed in a *spoll-da* hypomorph at high temperature, neither of these possibilities is likely.

A third possibility is that homologs segregate via distributive disjunction at higher temperature, as occurs in *D. melanogaster* (Grell, 1963). Distributive disjunction has also been shown in yeast strains monosomic for chromosomes I and III and monosomic for chromosome I where the chromosome was bisected into two functional fragments (Guacci and Kaback, 1991). In the case of distributive disjunction, chromosomes segregate without the necessity of crossovers. If distributive disjunction were the mechanism by which spore

viability is rescued in *spo11-da* cells is rescued at high temperature, the expectation would be that a *spo11-yf* strain would also exhibit rescued spore viability at high temperature. To address this issue, I dissected tetrads in of both *spo11-da* and *spo11-yf* mutants from liquid cultures incubated at 30ºC and 34.5ºC. In this experiment, the *spo11-da* strain's spore viability increased from 30% to 83% at 30°C and 34.5°C, respectively, whereas the *spo11*-yf strain exhibited <1% spore viability at both temperatures thus eliminating the possibility that chromosomes segregate via distributive disjunction in the absence of recombination. I cannot exclude the possibility, however, that activation of the distributive disjunction machinery depends on a base level of recombination initiation.

A final possibility is that viable spores are artificially selected in the process of preparing the cells for tetrad dissection. Since spores are formed at normal levels in these mutants but few intact tetrads are visible upon cell wall digestion with zymolyase, it may be that primarily cells that have undergone proper segregation survive this harsh treatment. Cell wall formation may be defective in cells that do not undergo proper segregation. Cell wall formation is linked to the proper attachment of spindle fibers to kinetochores and this essential step of nuclear division could be defective in *spo11-da* hypomorphs. If this is the case, then cells that have achieved proper nuclear divisions would be artificially selected for in our treatment protocol, with increased temperature exaggerating cell wall defects in cells that have undergone aberrant chromosome segregation.

4.5 Phosphorylation of histone H2A is required for normal meiotic progression.

One of the first detectable responses to DNA damage is phosphorylation of H2AX in the mouse model (Burma et al., 2001). ATM is recruited to the phosphorylation site, undergoes autophosphorylation and further activation in a positive feedback loop (Bakkenist

et al., 2003). Checkpoint response is linked to H2AX phosphorylation as ATM phosphorylates effector kinases such as Chk2, which phosphorylates targets that induce cell cycle arrest (Matsuoka et al., 2000) .

H2AX is quickly phosphorylated in response to the self-induced DSBs that occur in mouse meiosis. The γH2AX signal gradually disappears as DSBs are repaired and a second round of H2AX phosphorylation occurs in the unsynapsed regions of the XY pair of sex chromosomes (Mahadevaiah et al.,2001). This second round of phosphorylation remodels the chromatin in the sex chromosomes and silences transcription (Fernandez-Capitello, 2003).

In yeast, histone H2A has also been implicated in mitotic cell cycle response to DNA damage. H2A was shown to be phosphorylated across >50kb chromatin regions in the vicinity of a DSB induced by a site-specific endonuclease (Shroff et al., 2004). The checkpoint protein Rad9 has been shown to interact with phosphorylated H2A and its phosphorylation in G1 is phosphorylated-H2A dependent. Rad53 phosphorylation is also impaired in G1 in cells with non-phosphorylatable alleles of *H2A* (Hammet et al., 2007). Since H2AX is extensively phosphorylated, signaling DNA damage in mouse meiosis, it is reasonable to assume that the same is true of yeast meiosis, though this has not been directly observed.

To examine a role for H2A phosphorylation in the checkpoint function that is activated in response to low levels of DSBs, I introduced a non-phosphorylatable allele of *H2A* into a *spo11-da* strain. Surprisingly, meiotic progression was not accelerated in the absence of H2A phosphorylation. Instead, I found an additive effect of the *spo11-da* mutation with the H2A S129 mutation resulting in a more extensive delay.

The additional delay caused by non-phosphorylatable *H2A* may be due to an

53

inaccessibility of DSBs to repair proteins. In yeast, the INO80 chromatin remodeling complex is recruited to sites of DNA damage and is required for DNA damage-induced recombination (Van Atticum et al., 2004; Kawashima et. al, 2007). Yeast strains that lack INO80 are hypersensitive to many DNA damaging agents including MMS, suggesting a direct role in DSB repair (Kawashima et al., 2007). This may be because the INO80 complex remodels nucleosomes at the DSB site, allowing access of repair proteins (Tsukuda et al.,2005). Since my strain carries a mutation that renders H2A non-phosphorylatable, it is likely that INO80 dependent nucleosome removal is inefficient, since it requires H2A phosphorylation. In mammalian systems, though initial recruitment of repair proteins occurs independently of H2AX phosphorylation, γH2AX is required for full recruitment (Celeste et al.,2003). In the absence of INO80 in yeast mitotic cells, repair proteins such as Rad 51 cannot be recruited to form foci at these DSB sites (Falbo et al., 2009). If this is also true of meiosis, the process of homologous recombination would likely be inefficient, triggering a more extensive delay of progression when H2A phosphorylation is compromised.

Alternatively, lack of H2A phosphorylation may trigger a checkpoint in addition to that activated by the *spo11-da* mutation. This need not be mutually exclusive with the delayed repair theory. The checkpoint could be continually activated in response to the persistence of DSBs due to the lack of accessibility of repair proteins. The fact that the delay is present at all DSB levels supports the idea that this delay is independent of the *spo11-da* mutation and therefore DSB levels.

A third possible explanation for the delay is that, since sister chromatid repair is blocked by the inability to phosphorylate H2A, DSB repair is directed toward the homologue. H2A phosphorylation, along with H3K79 methylation mediate repair with the sister chromatid in mitotic yeast (Conde et al., 2009). Interhomolog repair is more time

54

consuming than IS repair (Goldfarb and Lichten, 2010), consistent with the delay I observed. Increased repair with the homologue would also explain the increase in spore viability in every *spo11* hypomorph *h2a* mutant relative to its isogenic strain with wild type *H2A*.

4.6 Isolation of HOP1 as a suppressor of Pch2 and/or Spo11 deficiency

As mentioned, the spo11-da mutation results in a protein that produces <20% of *SPO11* DSB levels. It has been proposed that Pch2 mediates phosphorylation of Hop1, which promotes the dimerization and activation of the Mek1 kinase that goes on to establish IH bias (Ho and Burgess, 2011; Niu et al., 2005; Carballo et al., 2008). When Pch2 is deleted in *spo11* hypomorphs, IH bias is reduced and a greater proportion of the available DSBs are repaired with the sister chromatid (N. Joshi, personal communication). The reduction in IH bias results in less crossover formation and therefore more chromosomes that missegregate in MI and thereby reduces spore viability (~1%). This low spore viability phenotype was easily detectable as a lack of microcolonies and provided a means to conduct a genetic screen. Rescue of the low spore viability resulted in visible colonies on leu- cyc media as outlined in the Results section.

Multicopy suppressor screens may identify three types of candidate: First, those that interact with the mutated protein in a complex, second, those that participate in the same pathway as the protein in question but lie downstream, third, those that lie in a parallel pathway and increase the output of that pathway. I expected candidates that fit those characteristics to increase DSB output and/or interact with Pch2 to enhance IH bias. I identified 79 initial candidates and a total of 7 final candidate plasmids that have been re-isolated from yeast (Table II). Of these, two were identified as plasmids that contain the *SPO11* gene and one has been sequenced that contains the *HOP1* gene.

While it is obvious that overexpression of WT Spo11 protein increases DSBs thus restoring DSBs that are repaired with the homologue, Hop1's role in promoting spore viability is less clear. Hop1 is a structural component of the SC axis that polymerizes along the length of chromosomes in MI. Yeast ATM/ATR-dependent phosphorylation of Hop1 promotes the dimerization and phosphorylation of the Mek1 kinase which, among other targets, phosphorylates Rad54 (Carballo et al., 2008; Niu et al., 2009). Rad54, a binding partner of Rad51, facilitates strand invasion of the sister chromatid by Rad51 (Sugawara et al., 2001). Rad54 inactivation is thus an important component of the barrier to homologous recombination with the sister chromatid and establishing IH bias in yeast (Niu et al., 2009). Hop1 is also required for normal levels of DSBs (Niu et al., 2005). Regions of the axis in which Hop1 protein is enriched are associated with greater levels of DSBs (Joshi et al., 2009). Hop1 deletion results in severely reduced spore viability in *S. cerevisiae* (Niu et al., 2005).

This function is highly conserved among many organisms. In the fission yeast *S. pombe*, Hop1 and Mek1 homologues promote homolog pairing and normal crossover formation. Spore viability in *hop1Δ mek1Δ* mutants was not reduced as severely as in *S. cerevisiae* (~83% in *S. pombe*). However, this may be attributable to the fact that there are only three chromosomes (vs. 16 in *S. cerevisiae*) and random segregation results in many spores that contain the full complement of chromosomes. DSBs were also deficient at a single hotspot in *S. pombe*, suggesting a conserved role in DSB formation. In mice, HORMA domain proteins 1 and 2 (orthologs of Hop1) have been implicated in DSB formation and CO control (Wojtasz et al., 2009). A conserved role for Trip13, the mouse homolog of Pch2, has also been demonstrated in mice and the normal deposition of HORMA domain proteins on chromosome axes is impaired in *trip13Δ* mutants.

HOP1 may alternatively genetically interact with *SPO11* in its role in normal DSB formation or its role in the establishment of the interhomologue bias. It is therefore unclear which of Hop1's activities result in the rescue of the low spore viability phenotype of *spo11-da pch2Δ* cells; more work will be necessary to elucidate Hop1's specific role in this rescue.

4.7 Concluding Remarks

The current work has revealed that poor spore viability and by inference chromosome missegregation at low DSB levels can be rescued by three apparently diverse factors. Higher than standard temperatures, a lack of histone H2 phosphorylation as well as Hop1 overexpression share in common that they result in high levels of spore viability in a *spo11* hypomorph. While the mechanisms for the restored spore viability are presently unknown, possible candidates include increased DSB formation, increased interhomolog bias and/or chromosome segregation mechanisms independent of recombination. This work has identified potential pathways by which functional gametes can be formed even when Spo11 function is compromised. Together, my findings reveal an unexpected plasticity of the meiotic chromosome segregation machinery in compensating for suboptimal DSB levels.

LITERATURE CITED

Ahuja, J. S. and Borner, G. V. (2011) Analysis of Meiotic Recombination Intermediates by Two-Dimensional Gel Electrophoresis. Methods of Mol. Biol. 2011; 745:99-116

Apping, D. R. (1999) Genetic Approaches to the Study of Protein-Protein Interactions. *Methods* **19**: 191-349.

Ausubel, F. M., Brent, R., Kingston, R. E., Moore, D. D., Seidman, J. G., Smith, J. A., and Struhl, K. ed. (2002) Short Protocols in Molecular Biology A compendium of Methods from Current Protocols in Molecular Biology. USA. Wiley and Sons.

Bakkenist, C. J. and Kastan, M. B. (2003) DNA Damage Activates ATM through Intermolecular Autophosphorylation and Dimer Dissociation. *Nature* **421:** 499-506.

Bhalla, N. and Dernberg, A. F. (2005) A conserved Checkpoint Monitors Meiotic Chromosome Synapsis in Caenorhabditis elegans. *Science* **310:** 1683-1686.

Burma, S., Chen, B. P., Murphy, M., Kurimasa, A., and Chen, D. J.(2001) ATM Phosphorylates Histone H2AX in Response to DNA Double-Strand Breaks. *The Journal of Biological Chemistry* **276**: 42,462-42,467.

Bzymek, M., Thayer, N. H., Oh, S. D., Kleckner, N. and Hunter, N. (2010) Double Holliday Junctions are Intermediates of DNA Break Repair. *Nature* **464**: 937-941.

Carballo, J. A., Johnson, A. L., Sedgwick, S. G., and Cha, R. S. (2008) Phosphorylation of the Axial Element Protein Hop1 by Mec1 Tel1 Ensures Meiotic Interhomolog Recombination. *Cell* **132**: 758-770

Celeste, A., Fernandez-Capitetillo, O., Kruhlak, M. J., Pilch, D. R., Staudt, D. W., Lee, A., Bonner, R. F., Bonner, W. M., and Nussenzweig, A. (2003) Histone H2AX Phosphorylation is Dispensable for the Initial Recognition of DNA Breaks. *Nature Cell Biology* **5**: 675-679.

Cha, R. S., Weiner, B. M., Keeney, S., and Kleckner, N. (2000) Progression of Meiotic DNA Replication is Modulated by Interchromosomal Interaction Proteins, Negatively by Spo11p and Positively by Rec8p. *Genes & Development* **14:** 493-503.

Choe, J., Kolodrubetz, D., and Grunstein, M.(1982) The Two Yeast Histone H2A Genes Encode Similar Protein Subtypes. *PNAS* **79**: 1484-1487.

Cimini, D. and Degrassi, F. Aneuploidy: a Matter of Bad Connections (2005). *Trends in Cell Biology* **15**: 442-451.

Conde, F., Refolio, E., Cordon-Preciado, V., Cortes-Ledesma, F., Aragon, L., Aguilera, A., and San-Segundo, P. A. (2009) The Dot1 Histone Methyltransferase and the Rad9

Checkpoint Adaptor Contribute to Cohesin-Dependent Double-Strand Break Repair by Sister Chromatid Recombination in Saccharomyces cerevisiae. *Genetics* **182**: 437-446.

Cuddihy, A. R. and OConnell, M. J. (2003) Cell-Cycle Responses to DNA Damage in G2. *Int. Rev. Cytol.* **222**: 99-140.

Diaz, R. L., Alcid, A. D., Berger, J. M., and Keeney, S. (2002) Identification of Residues in Yeast Spo11p Critical for Meiotic DNA Double-Strand Break Formation. *Molecular and Cellular Biology* **22:** 1106-1115.

Downs, J. A., Lowndes, N. F., and Jackson, S. P. (2000) A Role for Saccharomyces cerevisiae Histone H2A in DNA Repair. *Nature* **408**: 1001-1004.

Dresser, M. E., and Giroux, C. N. (1988) Meiotic Chromosome Behavior in Spread Preparations of Yeast. *The Journal of Cell Biology* **105**: 567-573.

Falbo, K. B., Alabert, C. Katou, Y., Wu, S., Han, J., Wehr, T., Xiao, J., He, X., Zhang, Z., Shi, Y., Shiragige, K., Pasero, P., and Shen, X. (2009) Involvement of a Chromatin Remodeling Complex in Damage Tolerance During DNA Replication. *Nature Structural Biology*, **16**: 1167-1172.

Falck, J. Coates, J. and Jackson, S. P. (2005) Conserved Modes of Recruitment of ATM, ATR, and DNA-PKcs to Sites of DNA Damage. *Nature* **434**: 605-611.

Fernandez-Capitello, O., Mahadevaieah, S. K., Celeste, A., Romanienko, P. J., Camerini-Otero, R. D., Bonner, W. M., Manova, K., Burgoyne, P., and Nussenzweig, A. (2003) H2AX is Required for Chromatin Remodeling and Inactivation of Sex Chromosomes in Male Mouse Meiosis. *Developmental Cell*, **4**: 497-508.

Gilbert, C. S., Green, C. M., and Lowndes, N. F. (2001) Budding Yeast Rad9 is an ATP-Dependent Rad53 Activating Machine. *Molecular Cell* **8:** 129-136

Goldfarb, T. and Lichten, M. (2010) Frequent and Efficient Use of the Sister Chromatid for DNA Double-Strand Break Repair during Budding Yeast Meiosis. *Plos Biology* **8**: 1-12.

Grell, E. H. (1963) Distributive Pairing of Compound Chromosomes in Females of Drosophila Melanogaster. *Genetics* **48**: 1217-1229.

Guacci, V. and Kaback, D. B. (1991) Distributive Disjunction of Authentic Chromosomes in Sacharomyces Cerevisiae. *Genetics* **127**: 475-488.

Hammet, A., Magill, C., Heierhorst, J., and Jackson, S. P.(2007) Rad9 BRCT Domain Interaction with Phosphorylated H2AX Regulates the G1 Checkpoint in Budding Yeast. *EMBO* **8**: 851-857.

Haruta, N., Kurokawa, Y., Murayama, Y., Akamatsu, Y., Unzai, S., Tsutsui, Y., and Iwasaki, H. (2006) The Swi5-Sfr1 Complex Stimulates Rhp51/Rad51- and Dmc1-mediated DNA Strand Exchange In Vitro. *Nature Structural& Molecular Biology* **13:** 823-830.

Henderson, K. A. and Keeney, S. (2004) Tying Synaptonemal Complex Initiation to the Formation and Programmed Repair of DNA Double-Strand Breaks. *PNAS* **101**: 4519-4524.

Ho, Hsuan-Chung and Burgess, S. M. (2011) Pch2 Acts through Xrs2 and Tel1/ATM to Modulate Interhomolog Bias and Checkpoint Function during Meiosis. *PLoS Genetics* **7:** 1-11.

Hunter, N. (2006). Meiotic Recombination. In, Molecular Genetics of Recombination, Aguilera, A. and Rothstein, R. (Eds), Topics in Current Genetics, Springer-Verlag, Heidelberg.

Jahaveri, A., Wysocki, R., Jobin-Robitaille, O., Altaf, M., Cote, J., and Kron, S. J. (2006) Yeast G1 Damage Checkpoint Regulation by H2A Phosphorylation is Independent of Chromatin Remodeling. *PNAS* **103:** 13771-13776.

Joshi, N., Barot, A., Jamison, C., and Borner, G. V. (2009) Pch2 Links Chromosome Axis Remodeling at Future Crossover Sites and Crossover Distribution during Yeast Meiosis *PLoS Genetics* **5:** 1-19.

Joyce, E. F., and McKim, K. S.(2009) Drosophila PCH2 Is Required for a Pachytene Checkpoint That Monitors Double-Strand-Break-Independent Events Leading to Meiotic Crossover Formation. *Genetics* **181:** 39-51

Joyce, E. F., McKim, K. S., (2010) Chromosome Axis Defects Induce a Checkpoint-Mediated Delay in Interchromosomal Effect on Crossing Over during Drosophila Meiosis. *PLoS Genetics* **6**: 1-14.

Kawashima, S., Ogiwara, H., Tada, S., Masahiko, H., Wintersberger, U., Enomoto, T., and Seki, M.(2007) The INO80 Complex is Required for Damage-Induced Recombination. *BBRC* **355**: 835-841.

Keeney, S., Giroux, C.N., and Kleckner, N. (1997) Meiosis-Specific DNA Double-Strand Breaks are Catalyzed by Spo11, a Member of a Widely Conserved Protein Family. *Cell* **88:** 375-384.

Kinner, A., Wu, W., Staudt, C., and Iliakis, G. (2008) γ-H2AX in Recognition and Signaling of DNA Double-Strand Breaks in the Context of Chromatin. *Nucleic Acids Research* **36**: 5678-5694.

Kobayashi, J., Tauchi, H., Sakamoto, S., Nakamura, A., Morishima, K., Matsuura S. et al. (2002) NBS1 localizes to gamma H2AX foci through interaction with the FHA/BRCT domain. *Current Biology* **12:** 1846-185.

Krogh, B. O. and Symington, L. S. (2004) Recombination Proteins in Yeast. *Annual Review of Genetics* **38:** 233-271.

Lee, K. (2004) The Signal from the Initiation of Recombination to the First Division of

Meiosis. *Eukaryotic Cell* **3:** 598-609

Li, Ji-Hoon and Paull, T. T. (2004) Direct Activation of the ATM Protein Kinase by the MRE11/Rad50/Nbs1 Complex. *Science* **304:** 93-96.

Mahadevaiah, S. K., Turner J. M. A., Baudat, F. Rogakou, E. P., de Boer, P., Blanco-Rodriguez, J., Jasin, M., Bonner, W. M., and Burgoyne, P. S. (2001) Recombinational DNA Double-Strand breaks in Mice Precede Synapsis. *Nature Genetics* **27:** 271-276.

Malone, R. E., Pansegrau, M., Foreman, K., Haring, S., Smith, S., Carpp, L., Houdek, D., Shah, B., and.

Martini, E., Diaz, R. L., Hunter, N., and Keeney, S. (2006) Crossover Homeostasis in Yeast Meiosis. *Cell* **126**: 285-295.

Matsuoka, S., Rotman, G, Ogawa, A., Shiloh, Y., Tamai, K., and Elledge, S. J. (2000) Ataxia Telangiectasia-Mutated Phospohorylates Chk2 in Vivo and in Vitro. *PNAS* **97**: 10389-10394.

Martini, E., Diaz, R. L. Hunter, N., and Keeney, S. (2006) Crossover Homeostasis in Yeast Meiosis. *Cell* **126**: 285-295.

Mcmahill, M. S., Sham, C. W., and Bishop, D. K. (2007) Synthesis Dependent Strand Annealing in Meiosis *Plos Biology* **5:** 2589-2601.

Naiki, T., Wakayama, T., Nakada, D., Matsumoto, K., Sugimoto, K. (2004) Association of Rad9 with Double-Strand Breaks Through a Mec1-Dependent Mechanism *Molecular Cell Biology* **24:** 3277-3285.

Nasmyth, K. A. and Tatchell, K. (1980) The Structure of Transposable Yeast Mating Type Loci. *Cell* **19**: 753-764.

Neale, M. J., and Keeney, S. (2006) Clarifying the Mechanics of DNA Strand Exchange in Meiotic Recombination. *Nature* **442**: 153-158.

Niu, H., Wan, L. Baumgartner, B., Schaefer, D. Loidl, J., and Hollingsworth, N. M. (2005) Partner Choice During Meiosis is Regulated by Hop1-promoted Dimerization of Mek1. *Molecular Biology of the Cell* **16**: 5804-5818.

Niu, H., Wan, L., Busygina, V., Kwon, Y., Allen, J. A., Li, X., Kunz, R. C., Kubota, K., Wang, B., Sung, P., Shokat, K. M., Gygi, S. P., and Hollingsworth, N. M. (2009) Regulation of Meiotic Recombination via Mek1-Mediated Rad54 Phosphorylation. *Molecular Cell* **36:** 394-404.

Padmore, R., Cao, L., and Kleckner, N. (1991) Temporal Comparison of Recombinational and Synaptonemal Complex Formation During Meiosis in *S. cerevisiae*. *Cell* **66**:1239-12567.

Paull, T. T., Rogakou, E. P., Yamazaki, V., Kirchgessner, C. U., Gellert, M., and Bonner, W. M. (2000) A Critical Role for Histone H2AX in Recruitment of Repair Factors to Nuclear

Foci after DNA Damage. *Current Biology* **10**: 886-895.

PLNT4140 Introductory Cytogenetics Lecture 3, part 3 of 4. University of Manitoba Dept. of Plant Science website [Online]. Available: http://home.cc.umanitoba.ca/~frist/PLNT3140/l03/l03.3.html. 3-2-2013.

Prieler, S. Penkner, A., Borde, V., and Klein, F. (2005) The Control of Spo11's Interaction with Meiotic Recombination Hotspots. *Genes and Development* **19**: 255-269.

Richmond, T. J., Finch, J. T., Rushton, B., Rhodes, D., and Klug, A. (1984) The Structure of the Nucleosome Core Particle. *Nature* **311**: 532-537

Rogakou, E.P., Pilch, D. R., Orr, A. H., Ivanova, V. S., and Bonnert, W. M. (1998) DNA Double-stranded Breaks Induce Histone H2AX Phosphorylation on Serine 139. *The Journal of Biological Chemistry* **273:** 5858-5868

San-Segundo, P. A. and Roeder, G. S. (1999) Pch2 Links Chromatin Silencing to Meiotic Checkpoint Control. *Cell* **97:** 313-324.

Schwacha, A. and Kleckner, N. (1997) Interhomolog Bias during Meiotic Recombination: Meiotic Functions Promote a Highly Differentiated Interhomolog-Only Pathway. *Cell* **90**: 1123-1135.

Schwartz, M. F., Duong, J. K., Sun, Z., Morrow, J., Pradhan, D., and Stern, D. F. (2002) Rad9 Phosphorylation Sites Couple Rad53 to the Saccharomyces cerevisiae DNA Damage Checkpoint. *Molecular Cell* **9:** 1055-1065.

Shroff, R., Arbel-Eden, A., Pilch, D., Ira, G, Bonner, W. M., Petrini, J. H., Haber, J. E., and Licten, M. (2004) Distribution and Dynamics of Chromatin Modification Induced by a Defined DNA Double-Strand Break. *Current Biology* **14:** 1703-1711.

Storlazzi, A., Xu, L., Schacha, A., and Kleckner, N. (1996) Synaptonemal Complex (SC) Component Zip1 Plays a Role in Meiotic Recombination Independent of SC Polymerization Along the Chromosomes. *PNAS* **93:** 9043-9048.

Stucki, M., Clapperton, J. A., Mohammad, D., Yaffe, M. B., Smerdon, S. J., and Jackson, S. P. (2005) MDC1 Directly Binds Phosphorylated Histone H2AX to Regulate Cellular Responses to DNA Double-Strand Breaks. *Cell* **123:** 1213-1226.

Sugawara, N., Wang, X., and Haber, J. E. (2003) In Vivo Roles of Rad52, Rad 54, and Rad 55 Proteins in Rad51-Mediated Recombination. *Molecular Cell* **12**: 209-219.

Tay, Y. D., and Wu, L.(2010) Overlapping Roles for Yen1 and Mus81 in Cellular Holliday Junction Processing. *Journal of Biological Chemistry* **285**: 11427-11432.

Tsukuda, T., Fleming, A. B., Nickoloff, J. A., and Osley, M. A. (2005) Chromatin Remodelling at a DNA Double-strand Break Site in Saccharomyces Cerevisiae. *Nature* **438**: 379-383.

Vader, G., Blitzblay, H. G., Tame, M. A, Falk, J. E., Curtin, L., and Hochwagen, A. (2011) Protection of Repetitive DNA Borders from Self-Induced Meiotic Instability. *Nature* **477**: 115-121.

Van Atticum, H., Fritsch, O., Hohn, B., and Gasser, S. M. (2004) Recruitment of the INO80 Complex by H2A Phosphorylation Links ATP-Dependent Chromatin Remodeling with DNA Double-Strand Break Repair. *Cell* **119**: 777-788

Weinert, T. A. and Hartwell, L. H. (1988) The RAD9 Gene Controls the Cell Cycle Response to DNA Damage in Saccharomyces cerevisiae. *Science* **241:** 317-322.

Woltering, D., Baumgartner, B., Bagchi, S., Larkin, B., Loidl, J., De los Santos, T., and Hollingsworth, N. M. (2000) Meiotic Segregation, Synapsis, and Recombination Checkpoint Functions Require Physical Interaction between the Chromosomal Proteins Red1p and Hop1p. *Molecular Cell Biology* **20:** 6646-6658.

Wu, H. and Burgess, S. M. (2006) Two Distinct Surveillance Mechanisms Monitor Meiotic Chromosome Metabolism in Budding Yeast. *Current Biology* **16**: 2473-2479.

Zanders, S., and Alani, E. (2009) The pch2Δ Mutation in Baker's Yeast Alters Meiotic Crossover Levels and Covfers a Defect in Crossover Interference. *PLoS Genetics* **5**:1-17.

Zanders, S., Brown, M. S., Chen, C., and Alani, E. (2011) Pch2 Modulates Chromatid Partner Choice During Meiotic Double-Strand Break Repair in Saccharomyces cerevisiae. *Genetics* **188**: 511-521.

APPENDICES

Yeast strains

SGY 13
MAT α ho::hisG spo11(Y135F)-HA3His6::KanMX4 CEN3::ADE2 his4-B ura3(Δsma-pst::hisG leu2::hisG ade2 lys5-P cyh2R can1S MET13B TRP5-S THR1-A CUP1R
MAT a ho::hisG spo11-HA3His6::KanMX4 CEN8::URA3 HIS4-B ura3(Δsma-pst::hisG LEU2 ade2 LYS5-P cych2S can1R met1 3B trp5-S thr1 - A cup1S

SGY 14 CUP1R
MAT α ho::hisG spo11(Y135F)-HA3His6::KanMX4 CEN3::ADE2 pch2::HygroX4 his4-B ura3(Δsma-pst::hisG leu2::hisG ade2 lys5-P, cyh2R can1S MET13B TRP5-S THR1-A
MAT a ho::hisG spo11-HA3His6::KanMX4 CEN8::URA3 pch2::HygroX4 HIS4-B ura3(Δsma-pst::hisG LEU2 ade2 LYS5-P cych2S can1R met1 3B trp5-S thr1 - A
cup1S

SGY 15
MAT α ho::hisG spo11(D290A)-HA3His6::KanMX4 CEN3::ADE2 his4-B ura3(Δsma-pst::hisG) leu2::hisG ade2 lys5-P cyh2R can1S MET13B TRP5-S THR1-A CUP1R
MAT a ho::hisG spo11(D290A)-HA3His6::KanMX4 CEN8::URA3 HIS4-B ura3(Δsma-pst::hisG LEU2 ade2 LYS5-P cych2S can1R met1 3B trp5-S thr1 - A cup1S

SGY16 CUP1R
MAT α ho::hisG spo11(D290A)-HA3His6::KanMX4 CEN3::ADE2 pch2::HygroX4 his4-B ura3(Δsma-pst::hisG leu2::hisG ade2 lys5-P, cyh2R can1S MET13B TRP5-S THR1-A
MAT a ho::hisG spo11(D290A)-HA3His6::KanMX4 CEN8::URA3 pch2::HygroX4 HIS4-B ura3(Δsma-pst::hisG LEU2 ade2 LYS5-P cych2S can1R met1 3B trp5-S thr1 - A
cup1S

SGY 48
MAT α ho::hisG spo11(D290A)-HA3His6::KanMX4 CEN3::ADE2 HIS4-B ura3(Δsma-pst::hisG leu2::hisG Cyc2R c24-S
MAT a ho::hisG spo11(D290A)-HA3His6::KanMX4 CEN3::URA3 his4-B ura3(Δsma-pst::hisG leu2::hisG cych2S c24-R

SGY 53
MAT a ho::hisG spo11(D290A)-HA3His6::KanMX4 CEN3::ADE2 pch2::HygroX4 his4-B leu2::hisG ade2 LYS5-P Cyc2S SGY 96

SGY 96
MAT α ho::hisG spo11(D290A)-HA3His6::KanMX4 CEN3::ADE2 pch2::HygroX4 his4-B leu2::hisG ade2 lys5-P Cyc2R

SGY 98
MAT α ho::hisG spo11(D290A)-HA3His6::KanMX4 CEN3::ADE2 pch2::HygroX4 his4-B leu2::hisG ade2 lys5-P Cyc2R
MAT a ho::hisG spo11(D290A)-HA3His6::KanMX4 CEN3::ADE2 pch2::HygroX4 his4-B leu2::hisG ade2 LYS5-P Cyc2S

SGY 108
MAT α ho::hisG spo11(D290A)-HA3His6::KanMX4 his4X::LEU2-(NgoMIV;ori)-URA3 ura3(Δsma-pst::hisG) leu2::hisG
MAT a ho::hisG spo11(D290A)-HA3His6::KanMX4 HIS4::LEU2-(NBam;ori) ura3(Δsma-pst::hisG)leu2::hisG

SGY 109
MAT α ho::hisG spo11(Y135F)-HA3His6::KanMX4 his4X::LEU2-(NgoMIV;ori)-URA3 ura3(Δsma-pst::hisG) leu2::hisG
MAT a ho::hisG spo11(Y135F)-HA3His6::KanMX4 HIS4::LEU2-(NBam;ori) ura3(Δsma-pst::hisG)leu2::hisG

SGY148
MAT α ho::hisG spo11(D290A)-HA3His6::KanMX4 his4X::LEU2-(NgoMIV;ori)-URA3 ura3(Δsma-pst::hisG) leu2::hisG
MAT a ho::hisG spo11(D290A)-HA3His6::KanMX4 HIS4::LEU2-(NBam;ori) ura3(Δsma-pst::hisG)leu2::hisG

SGY 149
MAT α ho::hisG spo11(D290A)-HA3His6::KanMX4 his4X::LEU2-(NgoMIV;ori)-URA3 ura3(Δsma-pst::hisG) leu2::hisG hta1S129A tha2 S129A
MAT a ho::hisG spo11(D290A)-HA3His6::KanMX4 his4X::LEU2-(NgoMIV;ori)-URA3 ura3(Δsma-pst::hisG) leu2::hisG hta1S129A tha2 S129A

SGY 150
MAT α ho::hisG spo11- HA3His6::KanMX4 HIS4::LEU2-(NBam;ori) ura3(Δsma-pst::hisG)leu2::hisG hta1S129A tha2 S129A
MAT a ho::hisG spo11(D290A)-HA3His6::KanMX4 his4X::LEU2-(NgoMIV;ori)-URA3 ura3(Δsma-pst::hisG) leu2::hisG hta1S129A tha2 S129A

SGY 151
MAT α ho::hisG spo11- HA3His6::KanMX4 HIS4::LEU2-(NBam;ori) ura3(Δsma-pst::hisG)leu2::hisG
MAT a ho::hisG spo11(D290A)-HA3His6::KanMX HIS4::LEU2-(NBam;ori) ura3(Δsma-pst::hisG) leu2::hisG

SGY 152
MAT α ho::hisG his4X::LEU2-(NgoMIV;ori)-URA3 his4-B ura3(Δsma-pst::hisG) leu2::hisG
MAT a ho::hisG HIS4::LEU2-(NBam;ori) his4-B ura3(Δsma-pst::hisG)leu2::hisG

SGY 153
MAT α ho::LYS2 ura3 leu2-K arg4-nsp,bgl hta1S129A, tha2S129A
MAT a ho::LYS2 ura3 leu2-R arg4-nsp,bgl hta1S129A tha2S129A

SGY 154
MAT α ho::hisG spo11(D290A)-HA3His6::KanMX4 pch2Δ::HygroX4 his4X::LEU2-(NgoMIV;ori)-URA3 ura3(Δsma-pst::hisG) leu2::hisG
MAT a ho::hisG spo11(D290A)-HA3His6::KanMX4 pch2Δ::HygroX4 HIS4::LEU2-(NBam;ori) ura3(Δsma-pst::hisG) leu2::hisG

VBY 1083
MAT α ho::hisG his4X::LEU2-(NgoMIV;ori)-URA3 his4-B ura3(Δsma-pst::hisG) leu2::hisG
MAT a ho::hisG HIS4::LEU2-(NBam;ori) his4-B ura3(Δsma-pst::hisG)leu2::hisG

Table 1: genotypes of all yeast strains used in this work.

Time Course	Genotype	Temperature	50% entry	Delay	Viability	Max divisions	Efficiency
TC10	SPO11	30C	6.8	n/a	91%	98%	n/a
	SPO11 h2a		6.8	0	100%	86%	88%
	spo11-da		8.6	1.8	40%	82%	83%
	spo11-da h2a		9.6	2.8	45%	84%	85%
	spo11-ha/da		6.6	-0.2	90%	92%	94%
	spo11-ha/da h2a		7.8	1	97%	94%	96%
	SPO11	33.5C	6.8	n/a	100%	80%	n/a
	SPO11 h2a		8	1.2	95%	64%	80%
	spo11-da		9.6	2.8	66%	78%	98%
	spo11-da h2a		10.2	3.4	92%	72%	90%
	spo11-ha/da		6.6	-0.2	84%	95%	119%
	spo11-ha/da h2a		7.6	0.8	94%	90%	>100%
TC 11	SPO11	30C	7.3	n/a	n.d	99%	n/a
	spo11-da		9	1.7	n.d.	94%	95%
	spo11-da pch2d		7.4	0	n.d.	94%	95%
	spo11-yf		7.3	0	n.d.	92%	92%
TC 12	SPO11	30C	7	n/a	93%	95%	n/a
	spo11-da		9.1	2.1	30%	95%	100%
	spo11-da pch2d		6.6	-0.4	0%	94%	99%
	spo11-yf		6.6	-0.4	0%	96%	101%
	SPO11	34.5C	10.4	n/a	99%	94%	n/a
	spo11-da		10.4	0	83%	76%	81%
	spo11-da pch2d		6	-4.4	0%	77%	82%
	spo11-yf		5.8	-4.6	0%	62%	66%
TC 13	SPO11	30	8	n/a	n.d	93%	n/a
	spo11-da		8.2	0.2	n.d.	77%	83%
	spo11-da		8.1	0.1	n.d	87%	94%
	spo11-da pch2d		6.3	-1.7	n.d.	84%	90%
	spo11-da pch2d		7.5	-0.5	n.d.	92%	99%
	spo11-yf		7	-1	n.d.	82%	88%
	spo11-yf		7.3	-0.7	n.d.	85%	91%

Table 2. Time course number, temperatures, 50% entry mark, delay/advancement relative to the WT strain, efficiency of nuclear divisions relative to the WT, and spore viability of all strains in all considered in this work. Note: The WT in TC 13 at 30°C was significantly delayed relative to the WT in all other time courses therefore it was considered an outlier and was not included in calculation of delays.